Sedimentary Evidence for the 2004 Sumatra Andaman Subduction Zone Earthquake

15-133

Jason R. Patton[1], Chris Goldfinger[1], Yusuf Djadjardihardja[2], Udrekh[2]
1. Oregon State University, College of Earth, Ocean and Atmospheric Sciences, 2. Badan Pengkajian Dan Penerapan Teknologi

Oregon State University · College of Earth, Ocean, and Atmospheric Sciences · BPPT · NSF

The paleoseismic history of earthquakes along subduction zones is an important tool to evaluate the cyclic hazards that millions of coastal residents are exposed to globally. We use litho- and chrono-stratigraphic methods to correlate turbidites between sediment cores in sedimentologically isolated accretionary prism slope basins and trench settings. In 12 of 15 cores collected in the region of the 2004 Sumatra-Andaman subduction zone earthquake, we interpret the uppermost turbidite to have been deposited as a result of seismic shaking related to this earthquake. Measures of relative age (lack of oxidation in the core tops, which can take months to a few years) and radiometric age (^{210}Pb and ^{14}C) support our interpretation of the uppermost turbidite. P Sequence (OxCal radiocarbon software) age modeling results in an age of -60 ± 10 cal yr BP 1950 (2010 ± 10 yr AD). These cores clearly show the ubiquitous generation of turbidity currents from this event. The physiographic setting precludes terrestrial or tsunami derived sources. The only remaining regional turbidity current triggers being random self-failure and earthquakes. High resolution (~ 25 cm) CHIRP subbottom data can resolve some multi-pulse coarse Bouma Tb-Tc beds in the ~three meter thick 2004 seismoturbidite. We find further evidence that there may be long-term cyclic repetition of large turbidites similar in size to the 2004 seismoturbidite.

Using our correlations for the stratigraphic history spanning the last 6.5 ka, we estimate recurrence of earthquakes capable of leaving a turbidite record in the region of the 2004 earthquake to be 260 ± 160 years. Down-core variations of interseismic intervals show similar trends between cores, supporting our correlations. Recurrence of trans-oceanic paleotsunami records in the northern Indian Ocean is between 280 and 320 years, consistent with our estimate, suggesting either coincidence, or similar sensitivity between tsunami and seismoturbidite preservation.

Plate Tectonic Setting

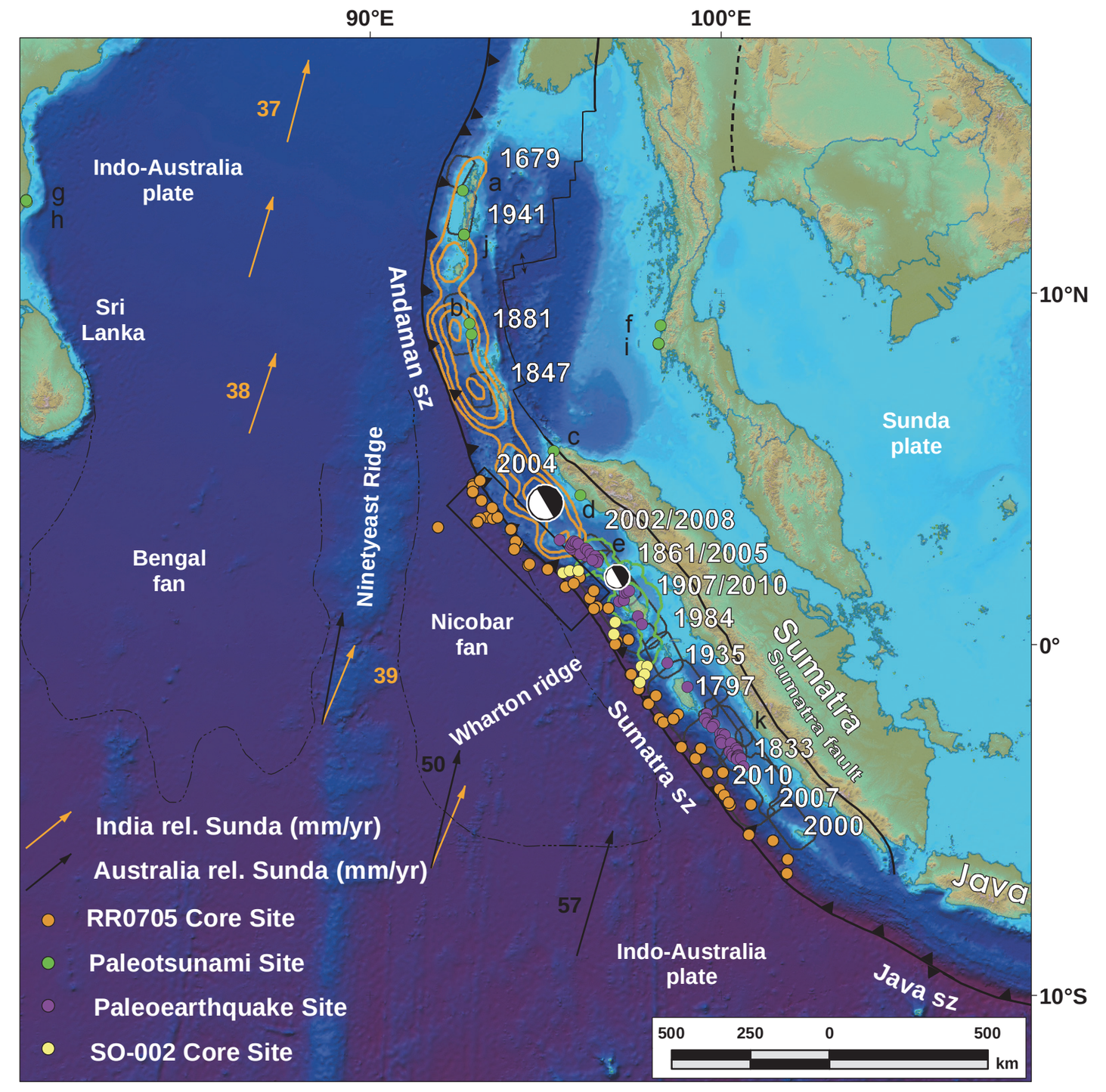

Earthquake Ground Motions Trigger Submarine Landslides

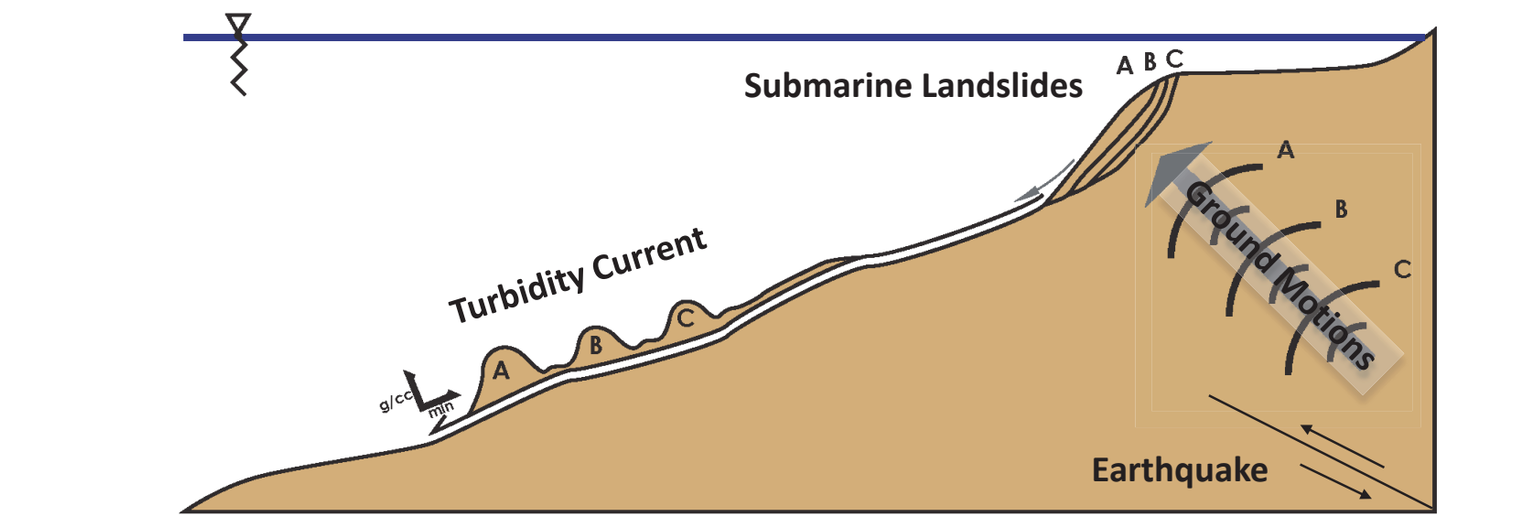

Sedimentary and Erosional Settings Offshore of Sumatra

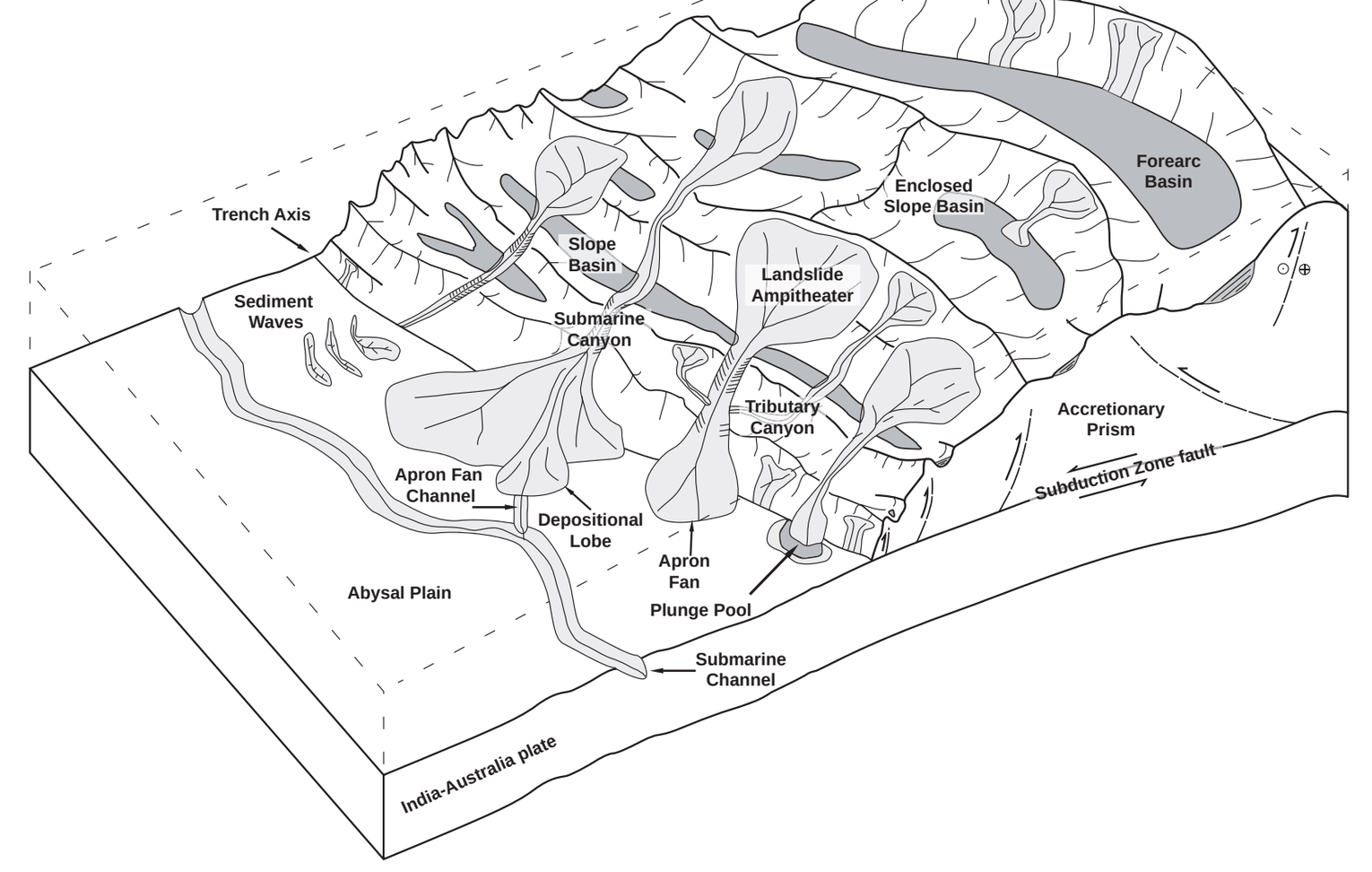

Core Sites Offshore of Sumatra

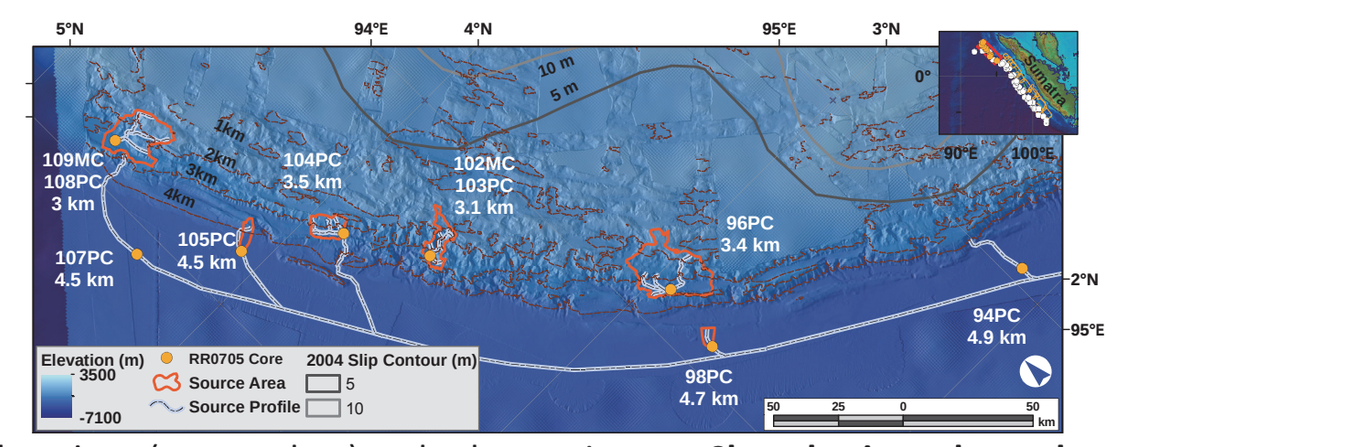

Core locations (orange dots) on bathymetric map. **Slope basin and trench source areas (orange)** were determined by outlining drainage divides surrounding all submarine topography contributing potential gravity flows to a given core site.

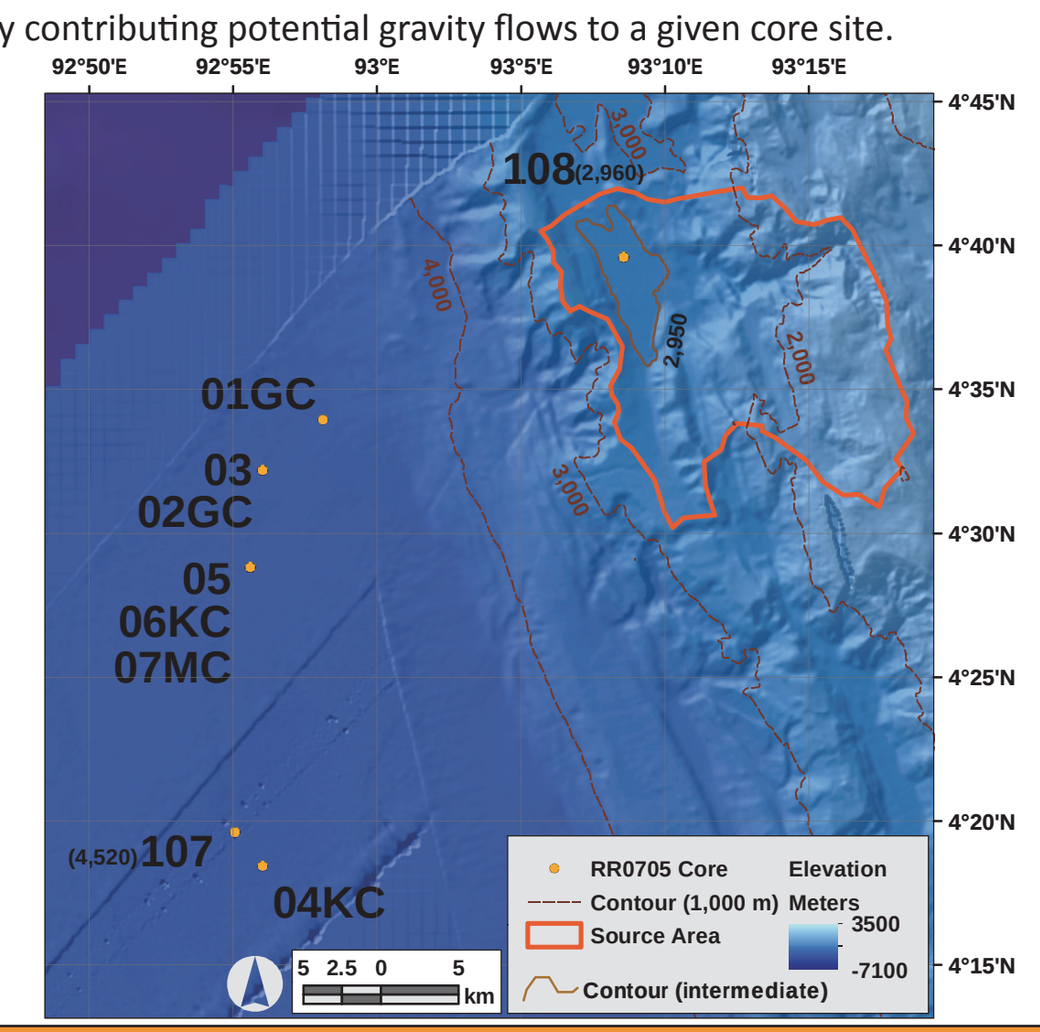

Shaded relief map showing **core sites 108 and 107 as orange dots**. Cores are labeled with their core number and the seawater depth at the core sites in meters.

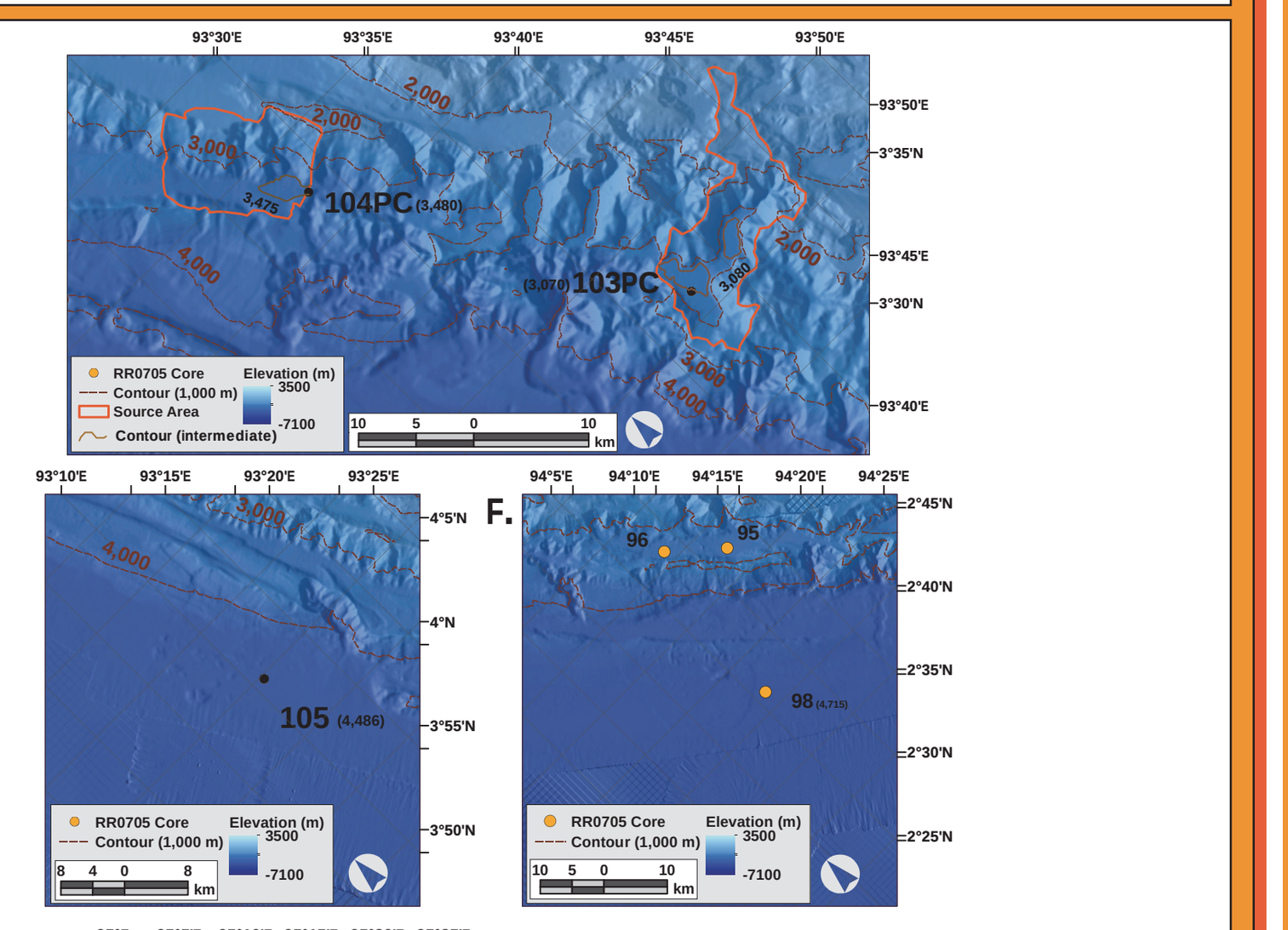

Core sites **103 and 104 are plotted as orange dots**, with the core depth in meters. Intermediate contours of 3,475 m and 3,080 m depict the shape of the basins. Core **105 is plotted** with the core depth in meters. Core **98 is plotted** with the core depth in meters. Core **94 is plotted** with the core depth in meters.

RR0705-96PC Core Site and Seismologic Record

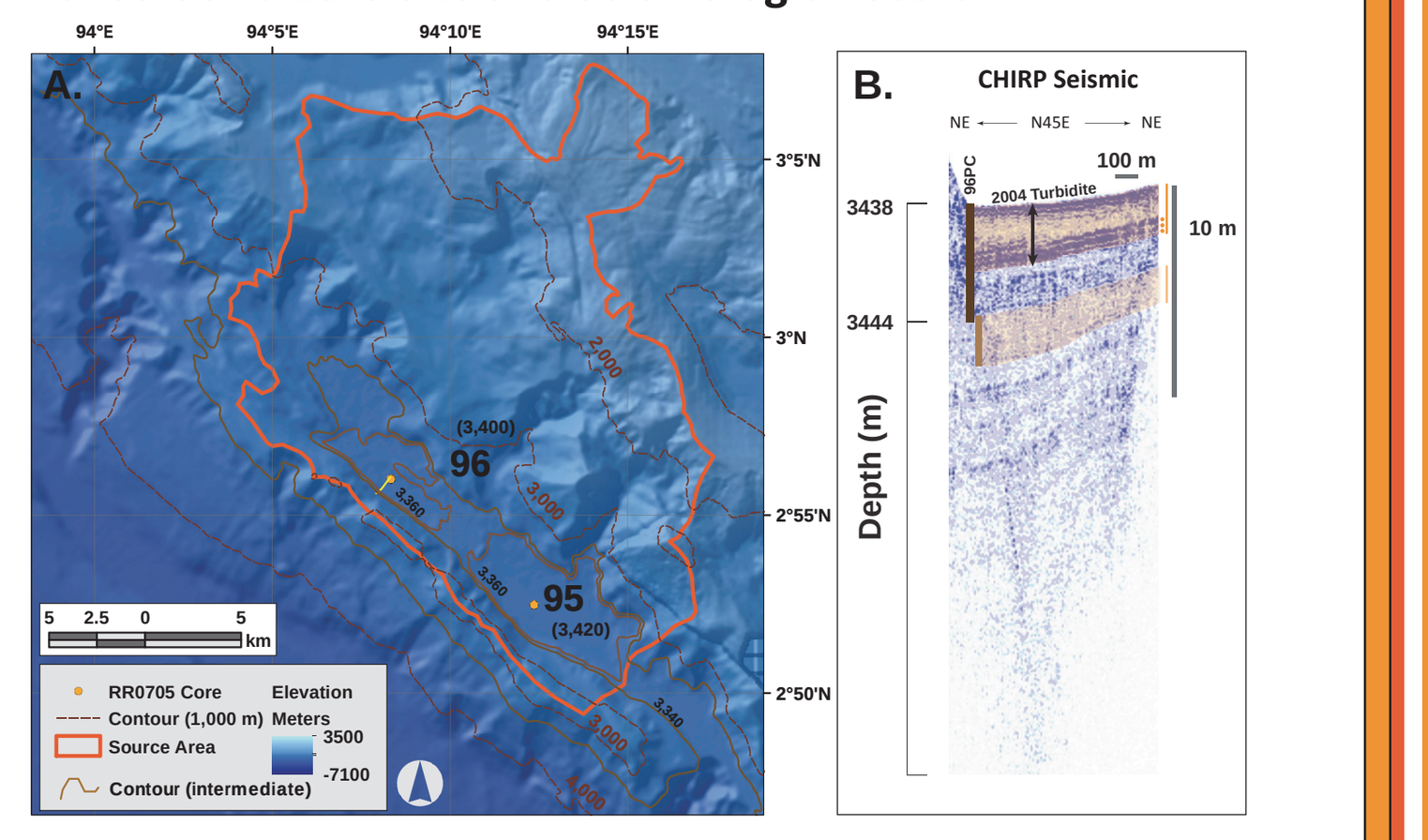

A. Core sites 96 and 95 are plotted as orange dots. Elevation contours are in meters. Intermediate contours of 3,360 m and 3,340 m depict the shape of the basins. The CHIRP seismic profile is plotted on the map as a yellow line crossing the core 96 core site. B. The CHIRP seismic profile crossing the basin at core 96. The core length of 96PC/TC is plotted in brown. Turbidite boundary interpreted in seismic data is overlain in transparent brown.

Possible Presence of 2004 & 2005 Turbidites

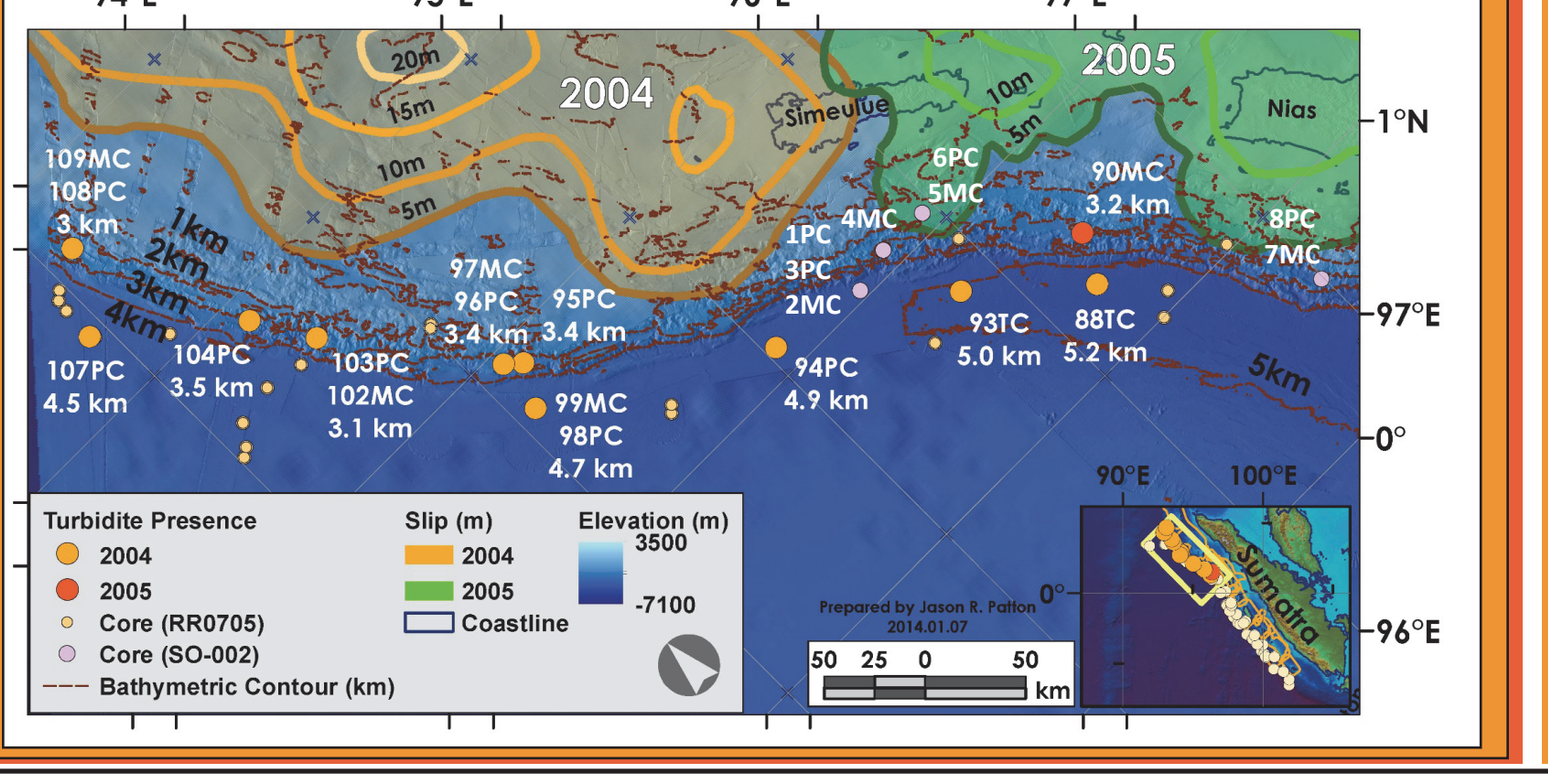

RR0705-96PC/TC

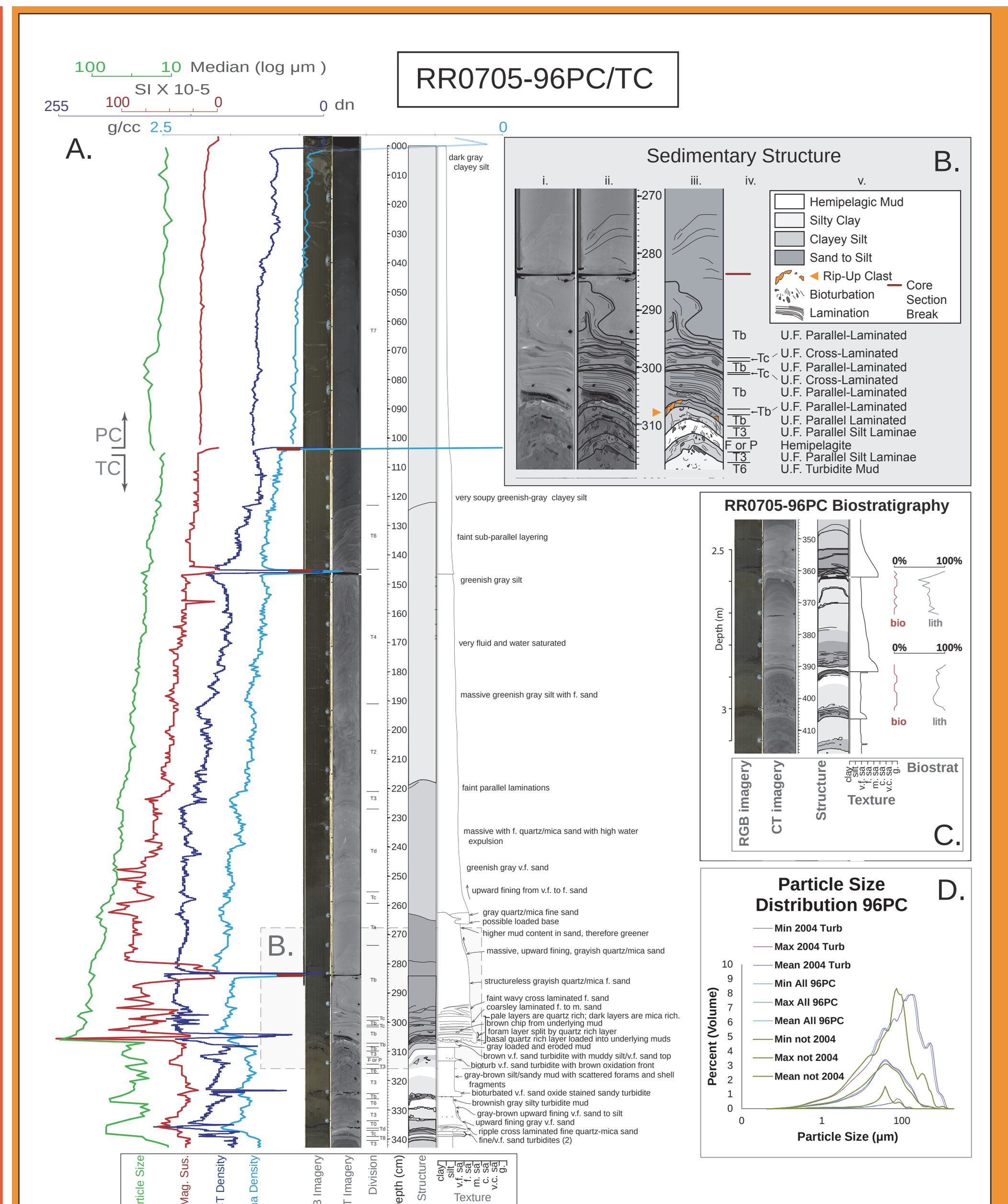

Key Observations to note:

- Soupy and unconsolidated sediments
- Lack of hemipelagic sediment in core tops
- Lack of oxidation in core tops (<1-5 years)

^{210}Pb Age Data

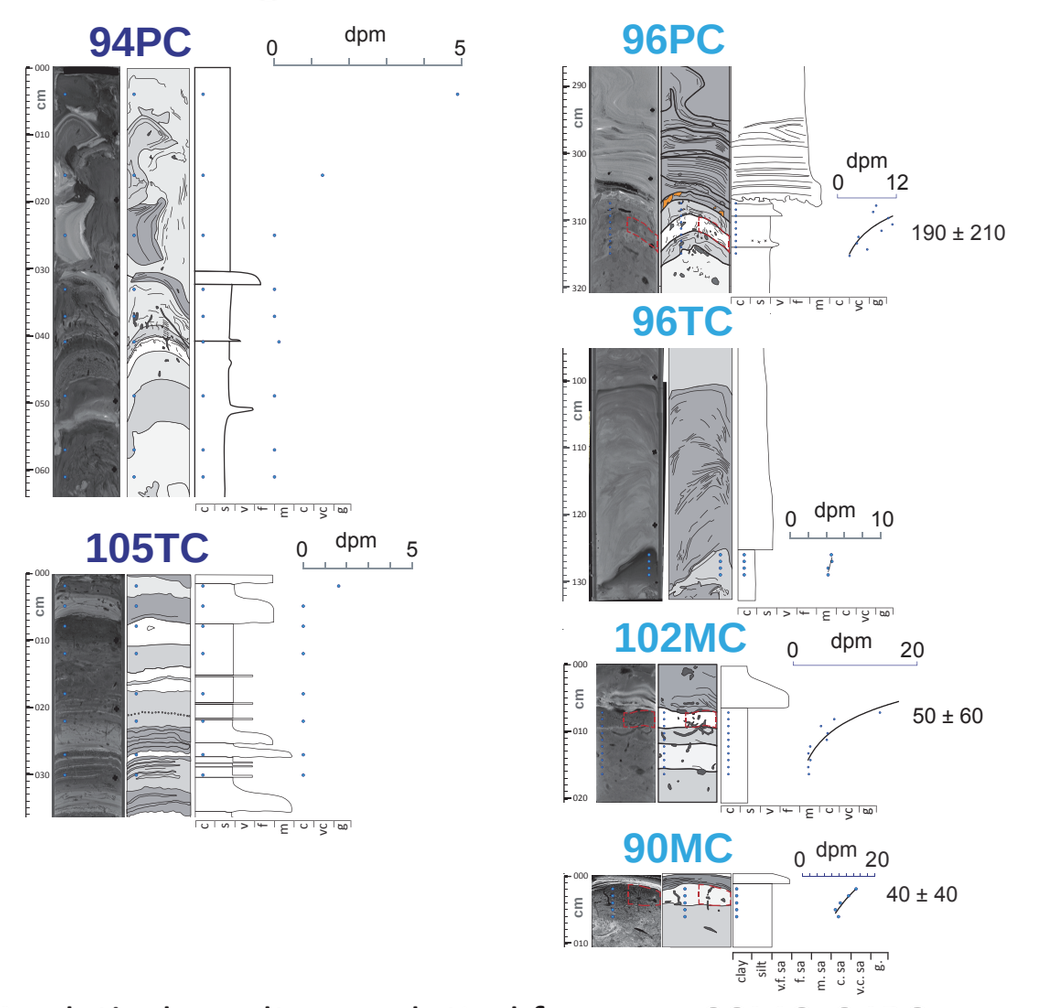

Analytical results are plotted for cores 90MC, 94PC, 96PC, 96TC, and 105TC. 210Pb decay per minute are plotted vs. depth with blue dots, alongside core data. Regressions are plotted for some cores. Core data include core depth (cm), CT imagery, turbidite structure, and sedimentary texture. ^{14}C ages are listed in cal yr BP with 95.4% error. Gray shaded ages are estimates based on our P_Sequence age model, discussed in the text. ^{14}C sample locations are outlined in dashed red lines

Comparison with Seismologic Data

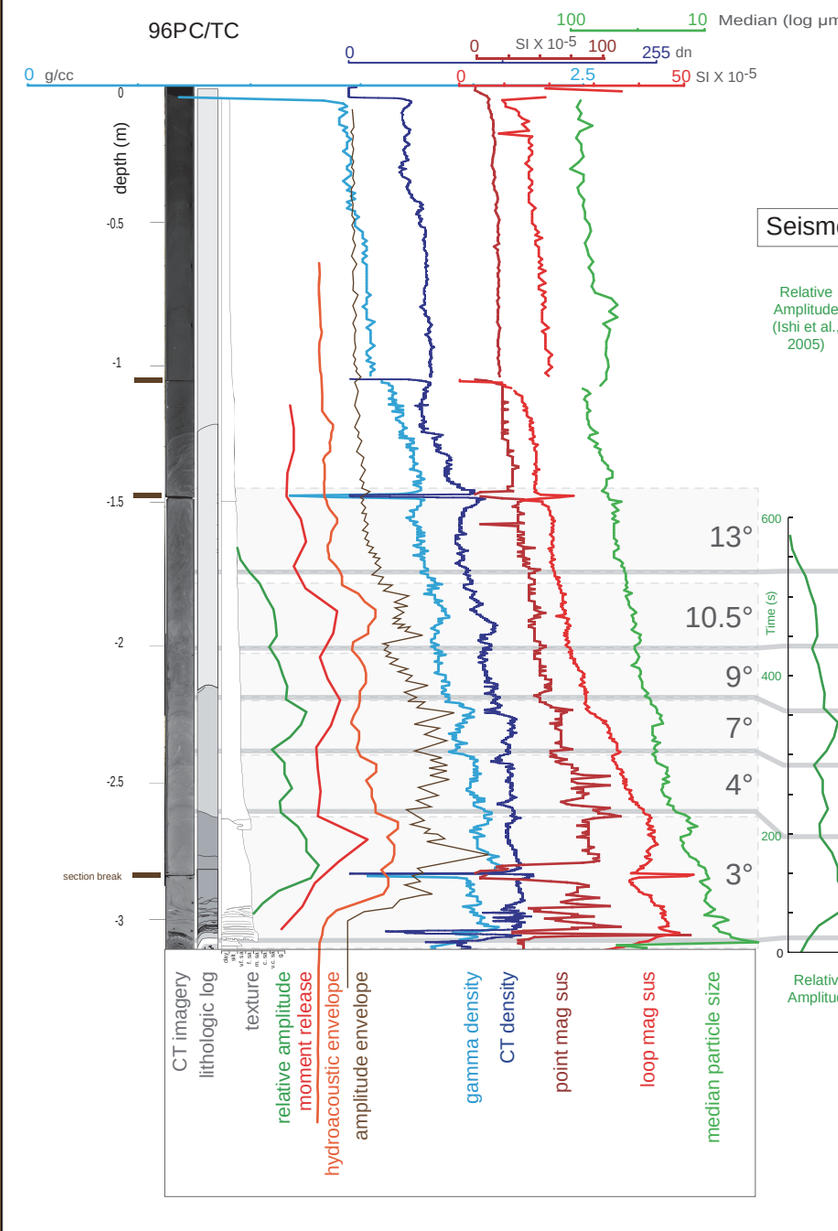

Core 96TC is scaled to 96PC and graphically spliced above 96PC to generate this composite core 96PC/TC. Moment release (vs. latitude) in red (Chlieh et al., 2007) and relative amplitude (vs. time) in green (Ishi et al, 2007), brown (Ni et al., 2005), and orange (Tolstoy and Bohnenstiehl, 2006) are plotted on the right, and scaled on the left, to match peaks in the loop ms data from composite core RR0705-96PC/TC. Thick grey tie-lines correlate the beginning of seismic peaks with each other and with base of peaks in the core geophysical data. Grey rectangles denote the correlation of the major pulses in the core geophysical data and the maxima for the seismic data. The rectangles are labeled with the latitude of the center of each slip patch maxima for the Chlieh et al. (2007) inversion model G-M9.15 (their figure 9).

Supporting Evidence for 2004 Seismoturbidite

	Simeulue study area			Nias study area		Batu study area				Earthquakes (magnitudes)
Core no.	2	4	5	7	9	11	12	14	16/18	
Setting	trench	slope basin	slope basin	slope basin	trench	slope basin	slope basin	slope basin	trench	
Potential 2004-05 turbidite?	yes	no	no	no	yes	no	no	no	yes	
years B.P. (0–200)	3 turbs in last 150 yr	18-23 yr (1 turb); 75-103 yr (3 turbs); 195-255 yr (1 turb)	no turbs in last 2795 - 3037 yr	no turbs in last 100-150 yr; 4 turbs older than 100-150 yr	at least 3 turbs in last 100-150 yr	no turbs in last 150 yr	no turbs in last 100- 150 yr	no turbs in last 100-150 yr; 5 turbs older than 100-150 yr	debrite in last 150 yr	2005 (M_w8.7); 2004 (M_w9.1); 1935 (M_w7.7); 1907 (M_w7.8); 1861 (M_w~8.5); 1797 (M_w~8.4)

(Sumner et al., 2013)

Possible 2004 Turbidite

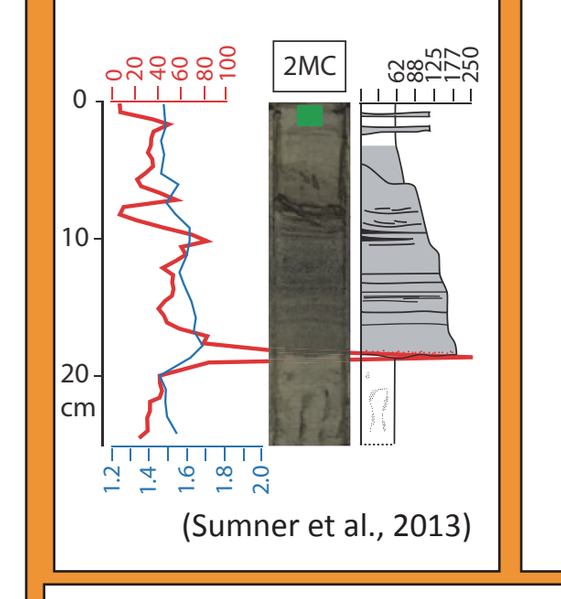

(Sumner et al., 2013)

RADIOCARBON AGES UNDERLYING THE UPPERMOST TURBIDITE IN CORES 96 AND 102.

Core	Sample Name	Lab Age	Error	Calibrated Age	Error	Sequence Age	Error	P_Sequence Age	Error
96PC	RR0705_96PC_206_208_SUM-227	480	20	-30	60	50	160	60	150
102MC	RR0705_102MC_065_075_SUM-249	460	20	40	40	50	60	na	na

Stratigraphic Correlation

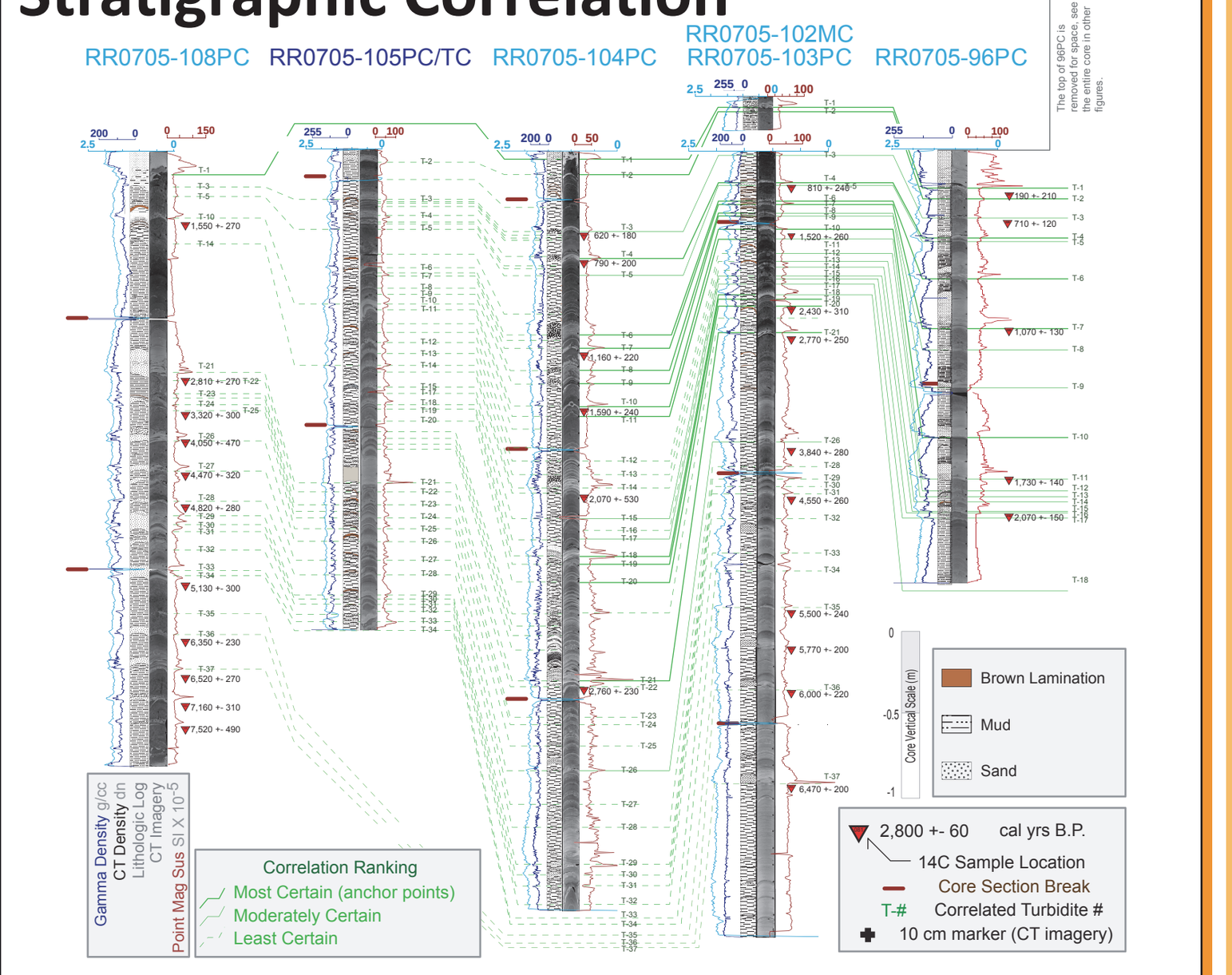

Space Time Relations for the Paleoseismic and Paleotsunami Record in the Northern Indian Ocean

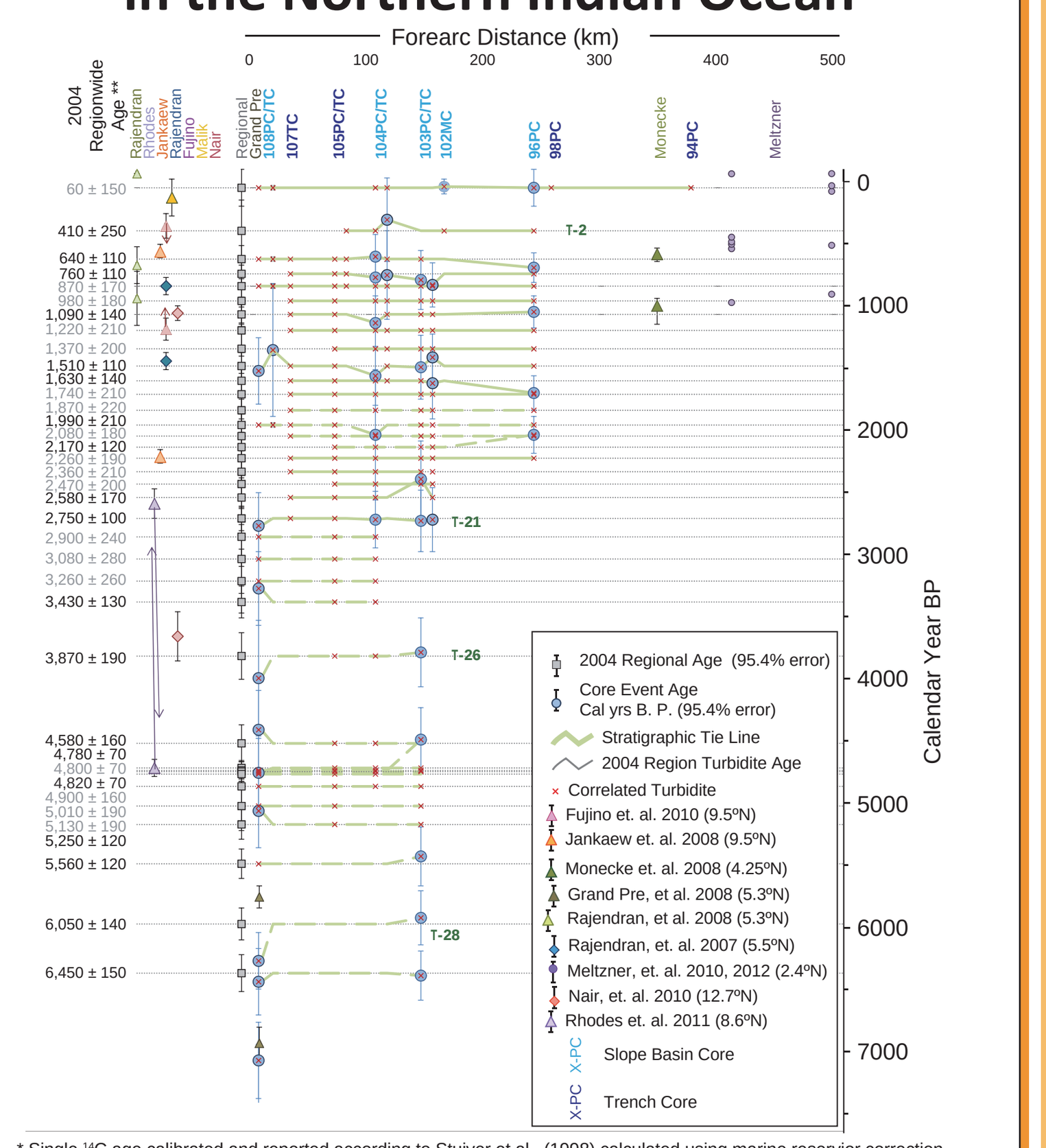

* Single ^{14}C age calibrated and reported according to Stuiver et al., (1998) calculated using marine reservior correction ($\Delta R = 16 \pm 78$). Error reported to 95.4%.
** Median age for each event, from Combine model. Grey ages are calculated with the "Date" OxCal command.
¥ OxCal v4.1.3 Bronk Ramsey (2009 a); Marine data from Reimer et al. (2009)

RADIOCARBON AGES AND PRESENCE/ABSENCE FOR REGIONAL TURBIDITES IN THE 2004 SUMATRA-ANDAMAN SUBDUCTION ZONE EARTHQUAKE REGION

Regional Turbidite Number	Analysis Type *	Source Core(s)	Regional Median Age (yrs BP) †	95% Error (yrs)	108	107	105	104	103	102	98 #	96	95	94 #
1	P_sequence	96PC	60	150	xx	--	--	xx	--	xx	xx	xx	xx	xx
2	R_date	104TC	410	250	--	--	x	xx	--	xx	--	xx	--	--
3	Combine	96PC,104PC	640	110	xx	x	x	xx	xx		--	xx	--	--
4	Combine	103TC,103PC,104TC,104PC	760	110	--	x	x	xx	xx		--	xx	--	--
5	Synthetic		870	170	xx	x	x	xx	xx		--	xx	--	--
6	Synthetic		980	180	--	x	x	xx	xx		--	xx	--	--
7	Combine	96PC,104PC	1,090	140	--	x	x	xx	xx		--	xx	--	--
8	Synthetic		1,220	210	--	x	x	xx	xx		--	xx	--	--
9	Synthetic		1,370	200	--	--	x	xx	xx		--	xx	--	--
10	Combine	103TC,103PC,104PC,108TC,108PC	1,510	110	xx	x	x	xx	xx		--	xx	--	--
11	Combine	96PC,103TC	1,630	140	--	x	x	xx	xx		--	xx	--	--
12	Synthetic		1,740	200	--	x	x	x	xx		--	xx	--	--
13	Synthetic		1,870	230	--	x	x	x	xx		--	xx	--	--
14	R_date		1,990	200	xx	x	x	x	xx		--	xx	--	--
15	Synthetic		2,080	180	--	x	x	xx	xx		--	xx	--	--
16	R_date	96PC	2,160	120	--	--	--	x	xx		--	xx	--	--
17	Synthetic		2,260	190	--	x	x	xx	xx		--	xx	--	--
18	Synthetic		2,360	210	--	x	x	xx	xx		--	x	--	--
19	Synthetic		2,470	200	--	--	x	xx	xx		--		--	--
20	R_date	103PC	2,580	160	--	x	x	xx	xx		--		--	--
21	Combine	103TC,103PC,104PC,108PC	2,750	100	xx	x	x	xx	xx		--		--	--
22	Synthetic		2,900	240	x		x	--	--		--		--	--
23	Synthetic		3,070	280	x		x	--	--		--		--	--
24	Synthetic		3,250	260	x		x	--	--		--		--	--
25	R_date	108PC	3,430	130	x		x	--	--		--		--	--
26	R_date	108PC	3,940	160	x		x	x	x		--		--	--
27	R_date	103PC	4,000	140	x		x	x	x		--		--	--
28	R_date	103PC	4,790	70	x		x	x	x		--		--	--
29	R_date	108PC	4,810	60	x		x	x	x		--		--	--
30	Synthetic		4,870	140	x		x	x	x		--		--	--
31	Synthetic		4,970	180	x		x	x	x					
32	Synthetic		5,060	190	x		x	x	x					
33	Synthetic		5,160	180	x		x		x					
34	R_date	108PC	5,250	120	x		x		x					
35	R_date	103PC	5,550	120	x				x					
36	R_date	103PC	6,050	130	x				x					
37	Combine	103PC,108PC	6,450	150	x				x					

* (1) R_date ages are the result of using the Sequence command in OxCal. (2) Combine are ages based on the "Combine" function in OxCal. (3) Synthetic ages are based on the "Date" command in our OxCal age model. Synthetic ages are not attributed to any "source" core.

† Calibrated age and errors reported to 95.4% error and are reported in calendar years. Calibrated age ranges before A. D. 1950 according to Stuiver and Reimer (1998) calculated using marine reservoir correction and regional delta R offset ($\Delta R = 16 \pm 78$).

§ The more certain that a regional turbidite is present in a given core is designated xx. The less certain that a regional turbidite is present in a given core is designated x. The absence of a correlated turbidite is designated --.

\# trench cores with sediments of low dynamic range, or greater coring deformation, are correlated with lesser certainty.

RECURRENCE INTERVAL (RI) ESTIMATES

Oldest Age/T-# *			Mean (Interseismic Time) §		
Core	R.I. (years)	S.D.	Core	R.I. (years)	S.D.
108	180	20	108	310	240
104	140	70	104	170	90
103	180	40	103	260	130
96	140	90	96	220	190
all cores #	160	50	all cores #	250	180

'* R.I. is calculated by dividing the age of the oldest turbdidite in each core by the regional T number for that core.
† R.I. is calculated by averaging the R.I. calculated at each turbidite that is calculated in the first three columns of this table.
§ R.I. is calculated by averaging the interseismic interval in each core.
\# The mean for "all cores" is the mean of the ages in that column (and an rms calculation of the standard deviation).

OVERALL SEDIMENTATION RATES

Core	Depth*	Error	Age †	Error§	Sed Rate #	Error**
108	344	1	7,520	490	0.46	0.07
104	445	1	4,290	120	1.04	0.03
103	380	1	6,470	200	0.59	0.03
96	400	1	2,070	150	1.93	0.09

* Depth of the deepest age in the core, in cm.
† The deepest calibrated age in the core with uncertainty reported to 95.4% error and reported in calendar years. Calibrated age ranges before A. D. 1950 according to Stuiver and Reimer (1998) calculated using marine reservoir correction and regional delta R offset ($\Delta R = 16 \pm 78$).
§ 95.4% Error in calendar years.
\# Sedimentation Rate in mm per year.
** Root Mean Square error

Slope Stability Force Balance

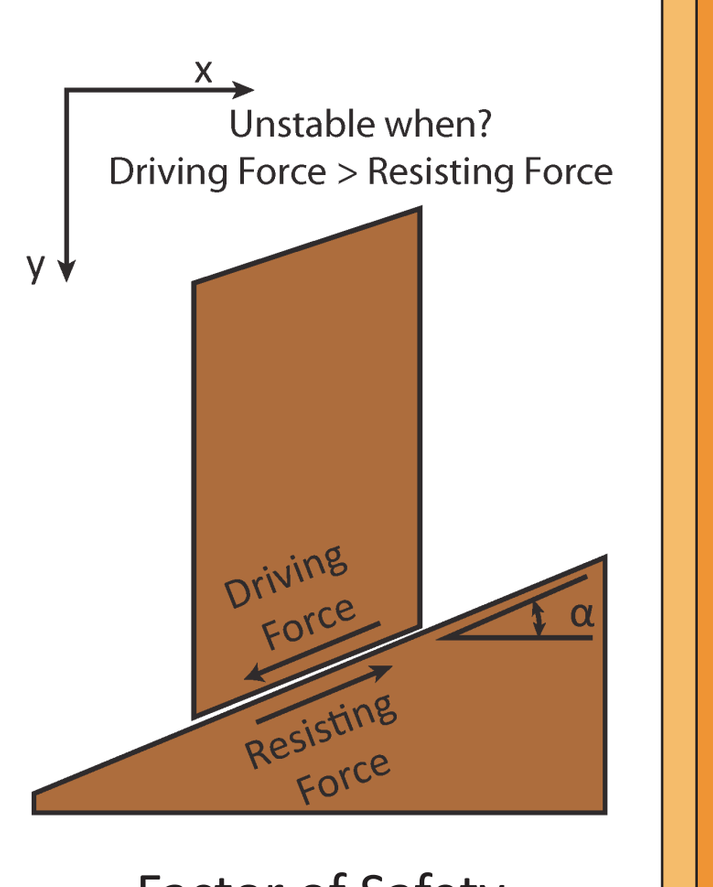

Factor of Safety
Stable: RF/DF > 1
Unstable: RF/DF < 1

Slope Stability Modeling

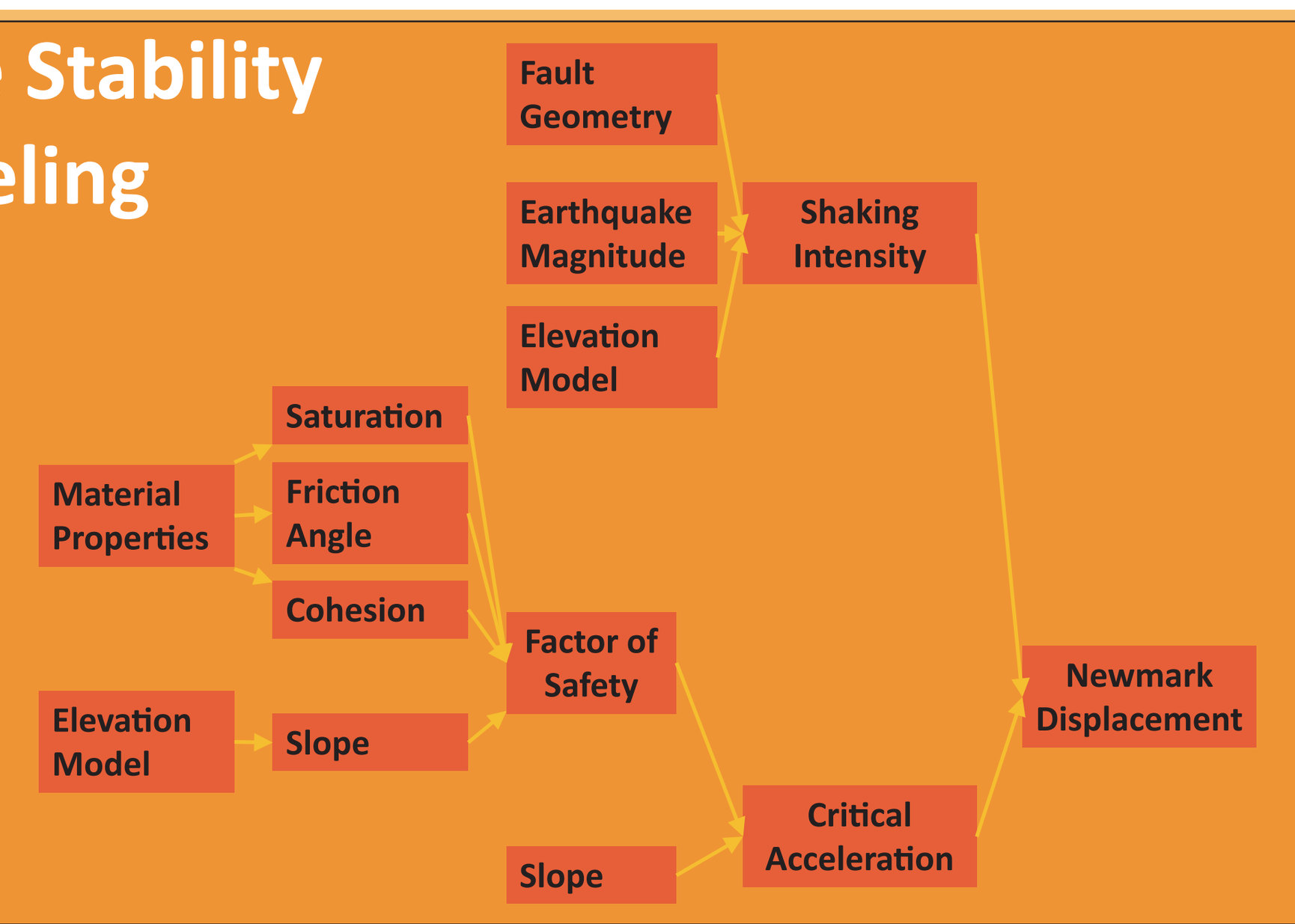

Earthquakes and Landslides

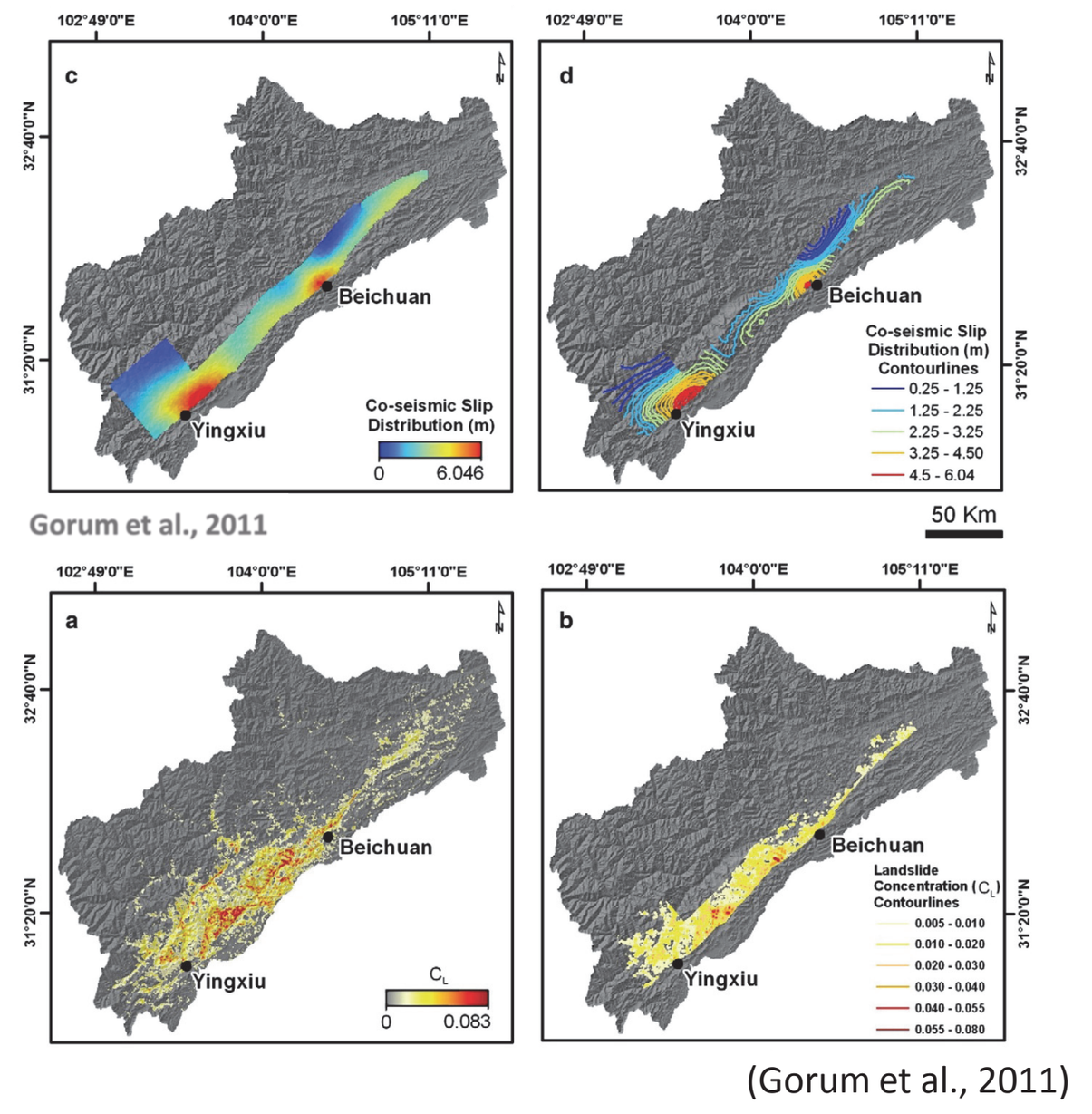

(Gorum et al., 2011)

Landslide Distance to Earthquakes

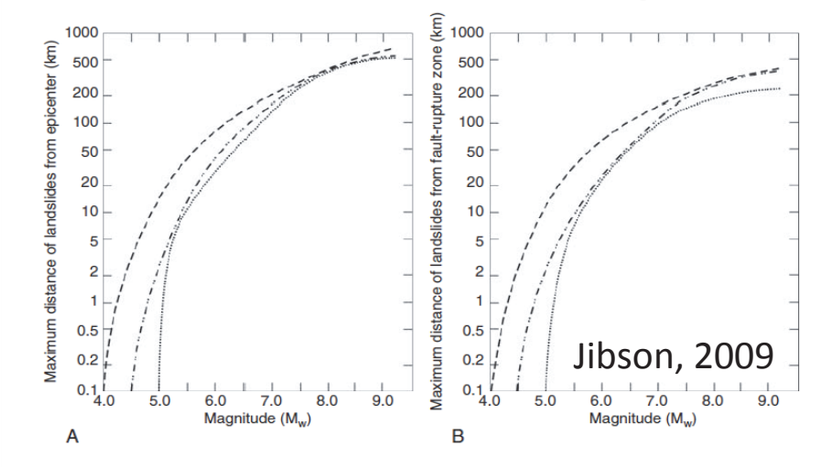

Upper Bound of maximum distance to landslides from (A) epicenter and (B) fault-rupture zone for earthquakes of different magnitudes.

- Dashed line is for disrupted slides and falls
- Dash-double-dot line is for coherent slides
- Dotted line is for lateral spreads and flows

Slip Inversion

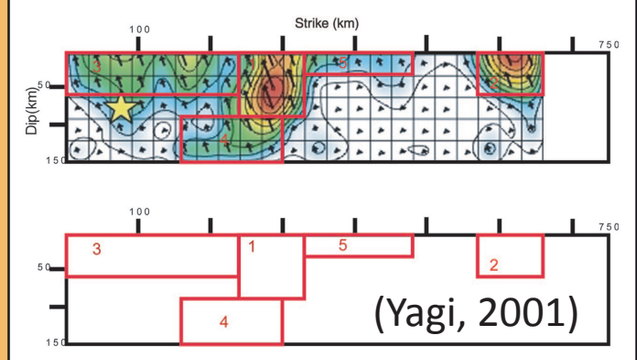

Area affected by Earthquake Triggered Landslides

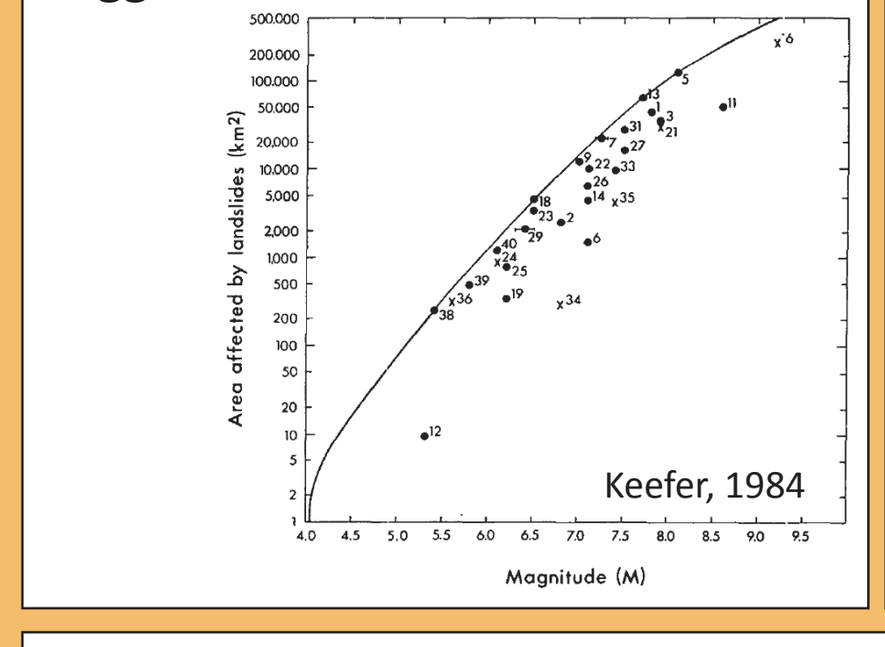

Simulated PGA: 2004 SASZ EQ

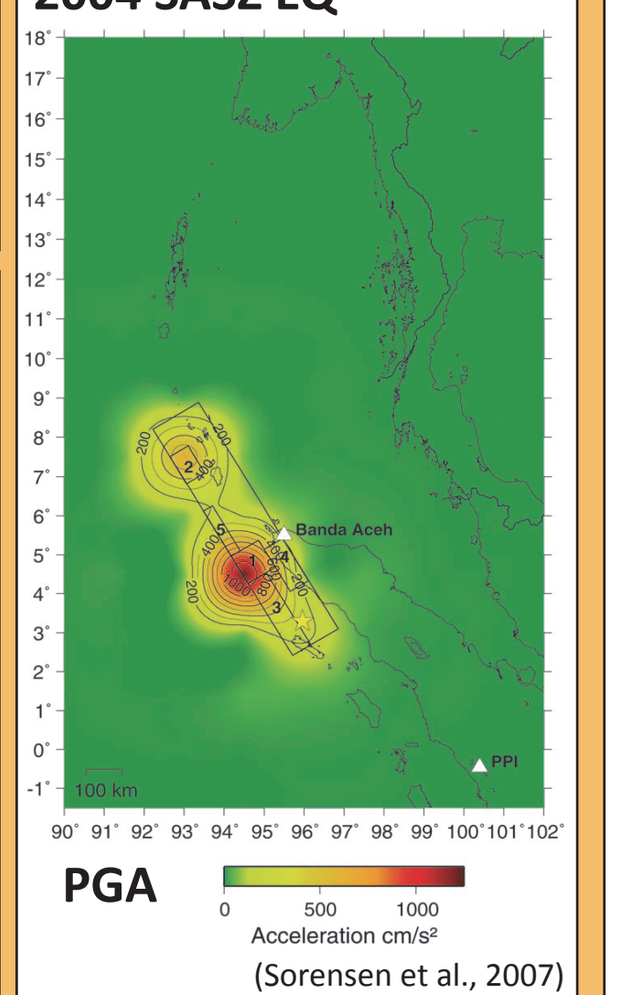

(Sorensen et al., 2007)

Ground Motion Attenuation Relations

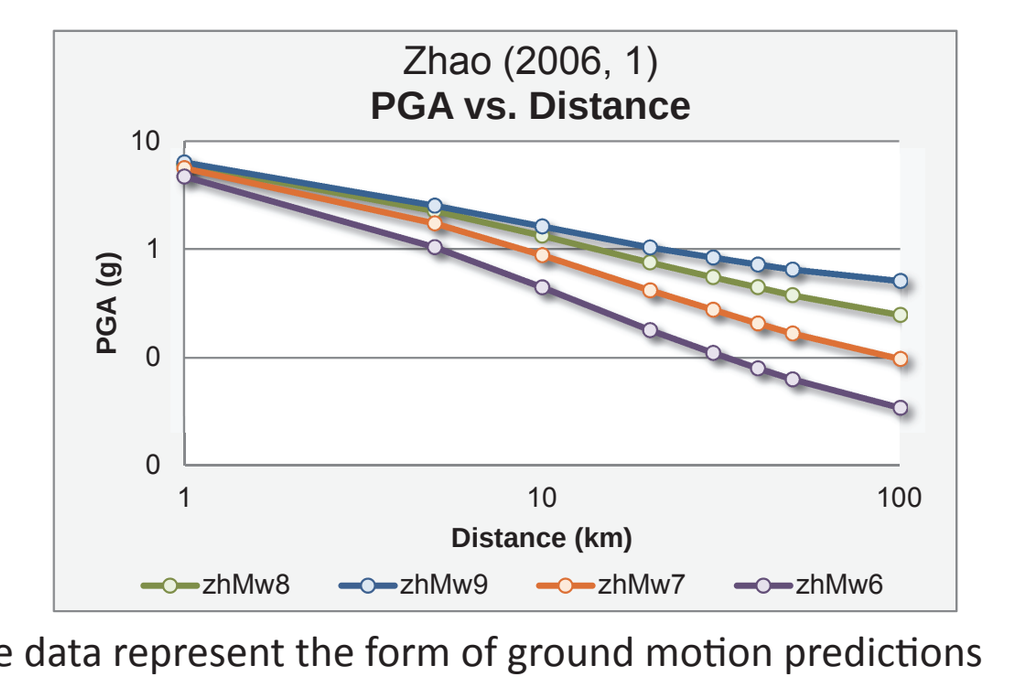

These data represent the form of ground motion predictions regressed by Zhao et al. (2006, equation 1), equation (2) for earthquakes of four magnitudes (M = 6, 7, 8, and 9 are purple, green, orange, and blue). "Distance" is the shortest distance between the ground surface and the fault plane (Rdist).

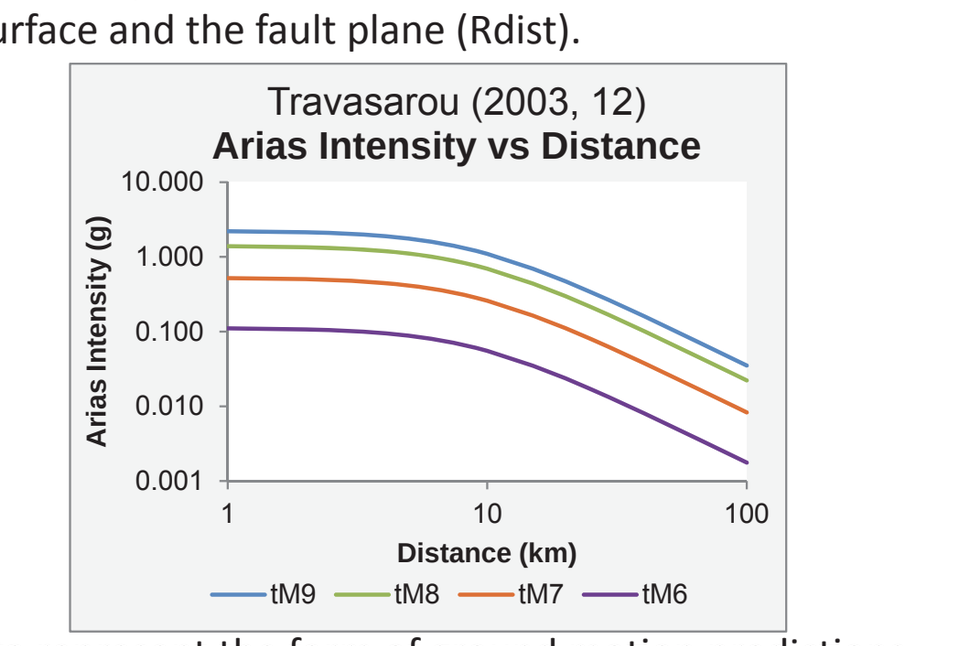

These data represent the form of ground motion predictions regressed by Travasarou et al. (2003, equation 12), equation (3) for earthquakes of four magnitudes (M = 6, 7, 8, and 9 are purple, green, orange, and blue).

Rdist (Fault Distance) Calculation

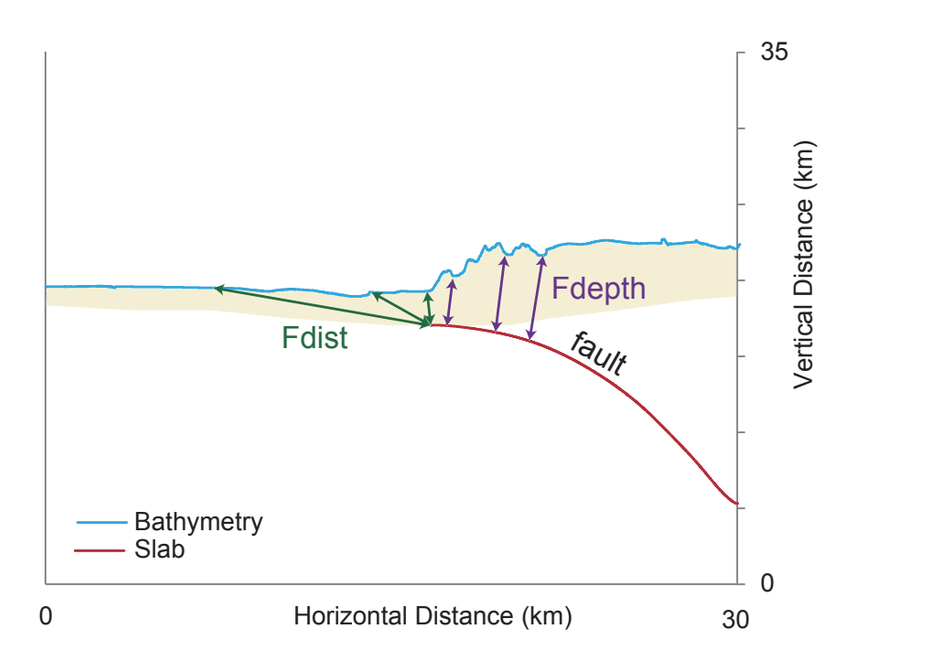

Seafloor bathymetry profile is plotted as a light blue line, the fault plane (slab) is plotted in red. Rdist is calculated by the length of Fdepth distances east of the trench (purple arrows) and Fdist distances west of the trench (green arrows).

Peak Ground Acceleration vs. Distance: Tohoku-Oki

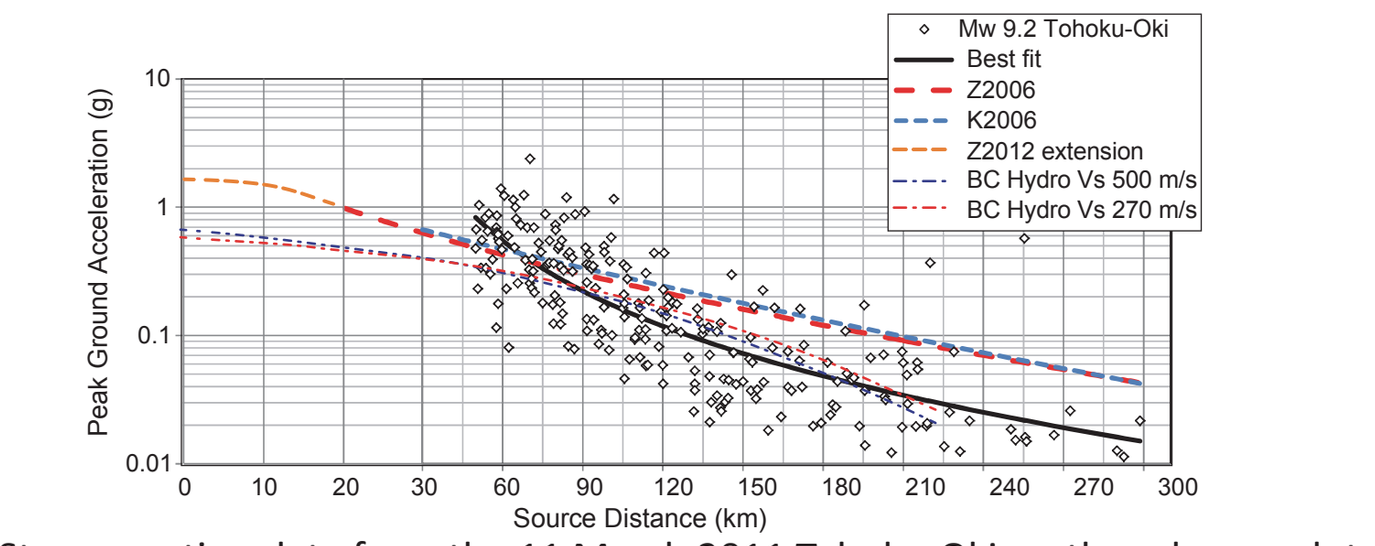

Strong motion data from the 11 March 2011 Tohoku-Oki earthquake are plotted as diamonds (Zhao et al., 2012) and ground motion predictions are plotted (Zhao et al., 2006 and 2012; Kanno et al., 2006; Abrahamson et al., 2014), modified from Zhao et al., 2012. Hypothetical extension of the mean regression line (Zhao et al. 2012) is plotted as an orange dashed line.

PGA and AI: Earthquakes M = 6, 7, 8, 9

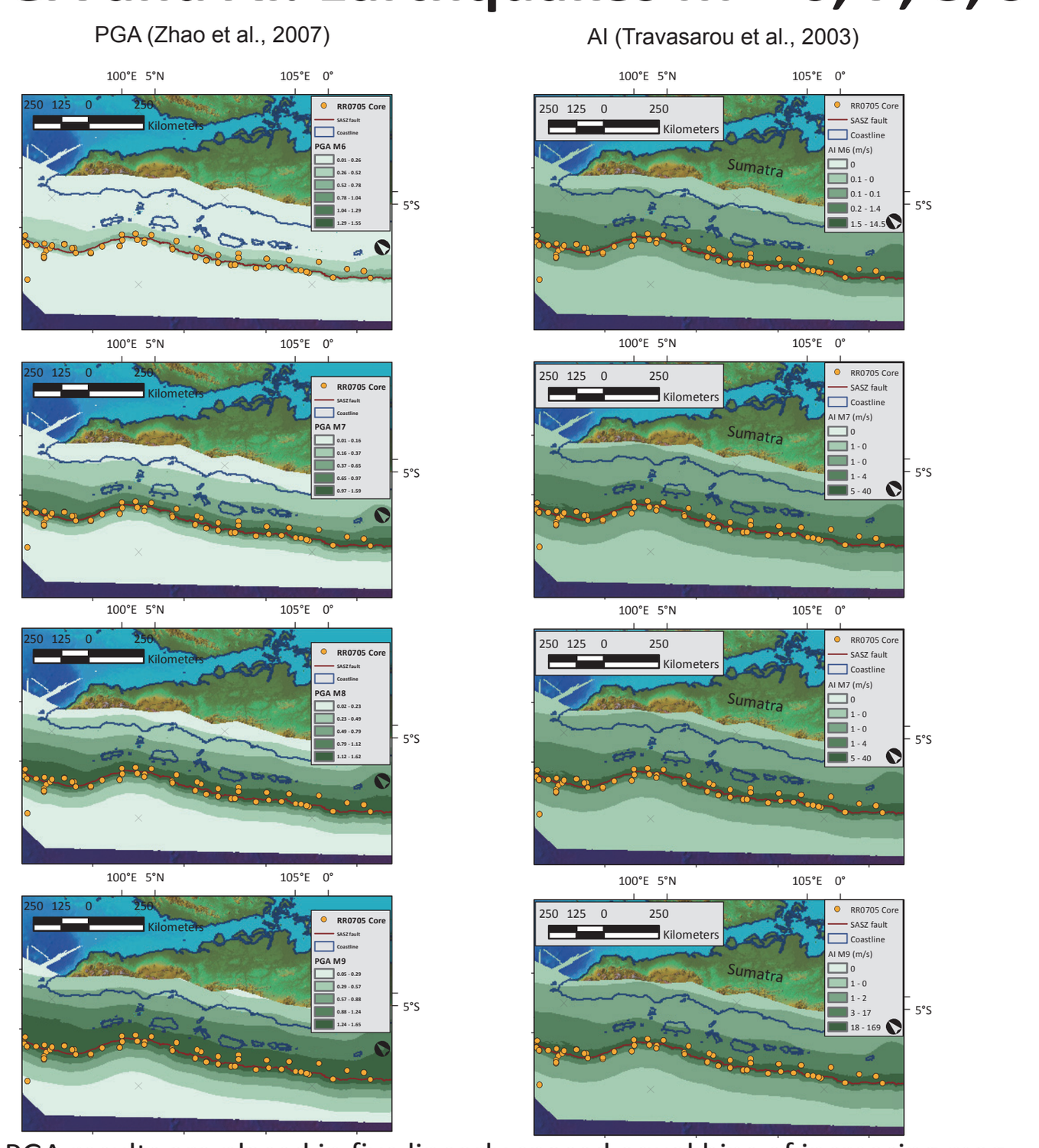

A. PGA results are placed in five linearly spaced equal bins of increasing magnitude as darker green. B. AI results are placed in five log10 spaced bins of increasing magnitude as darker green.

Newmark Displacement For Earthquakes of Magnitude M = 6, 7, 8, 9

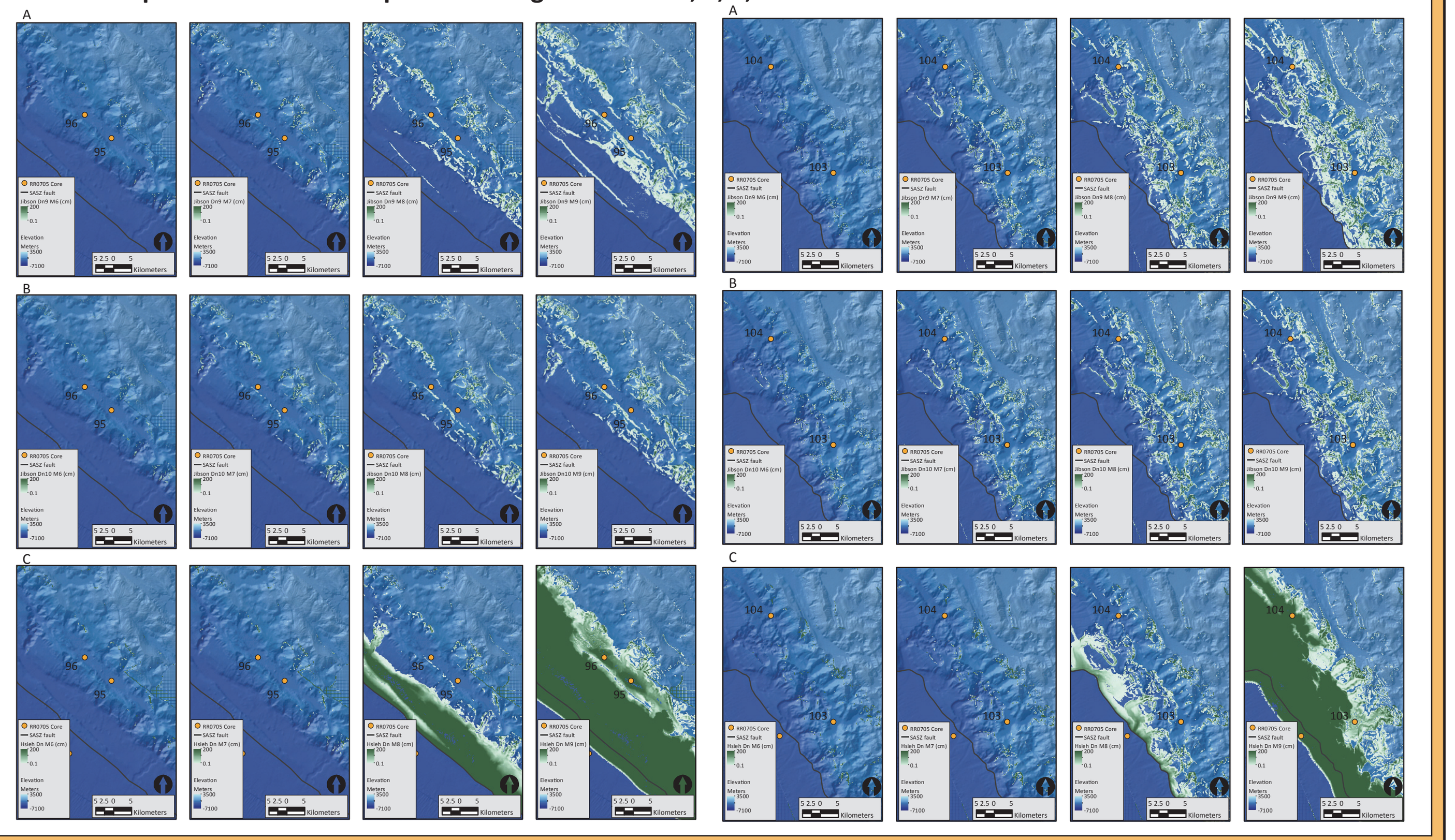

sFOS 2004 Earthquake

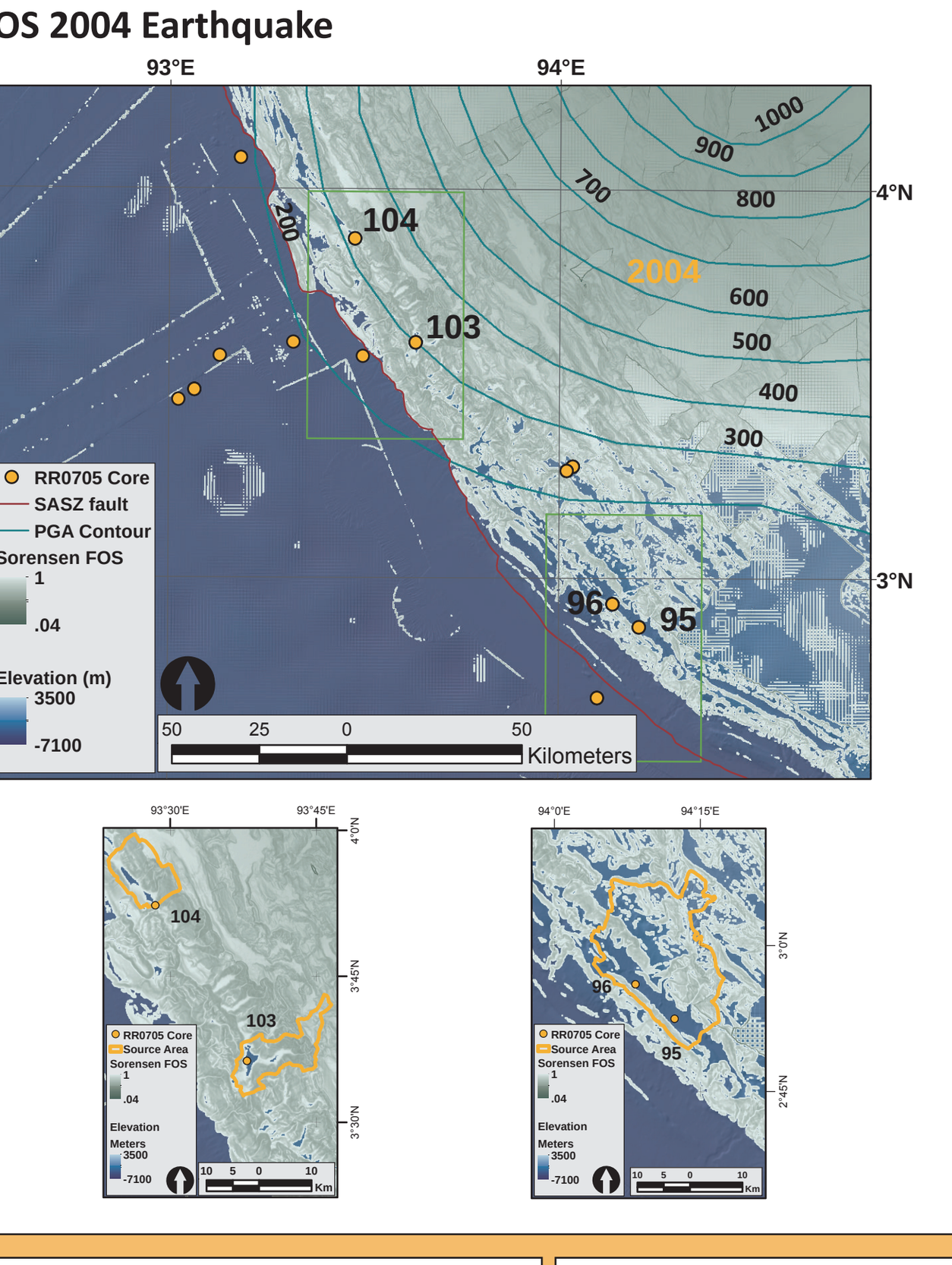

Slope Maps: Cores 95, 96, 103, 104

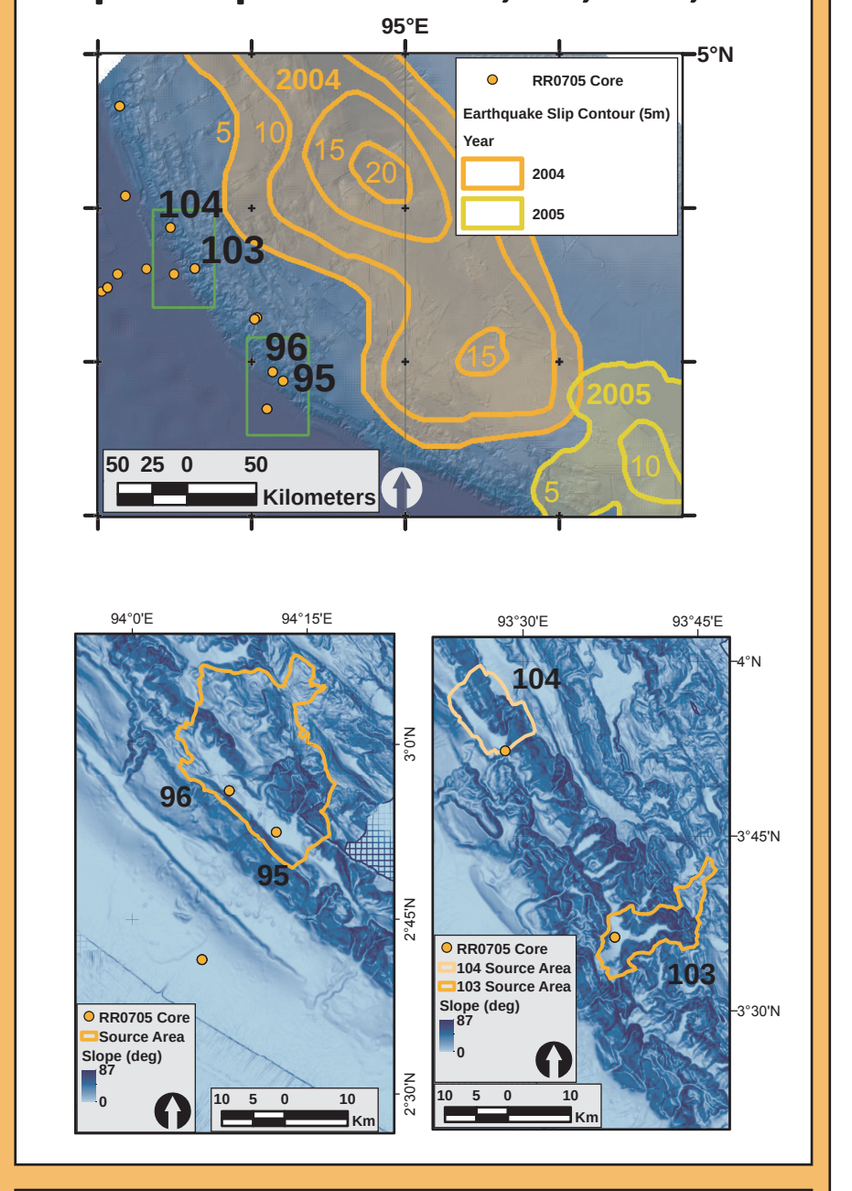

Rdist vs. PGA and AI

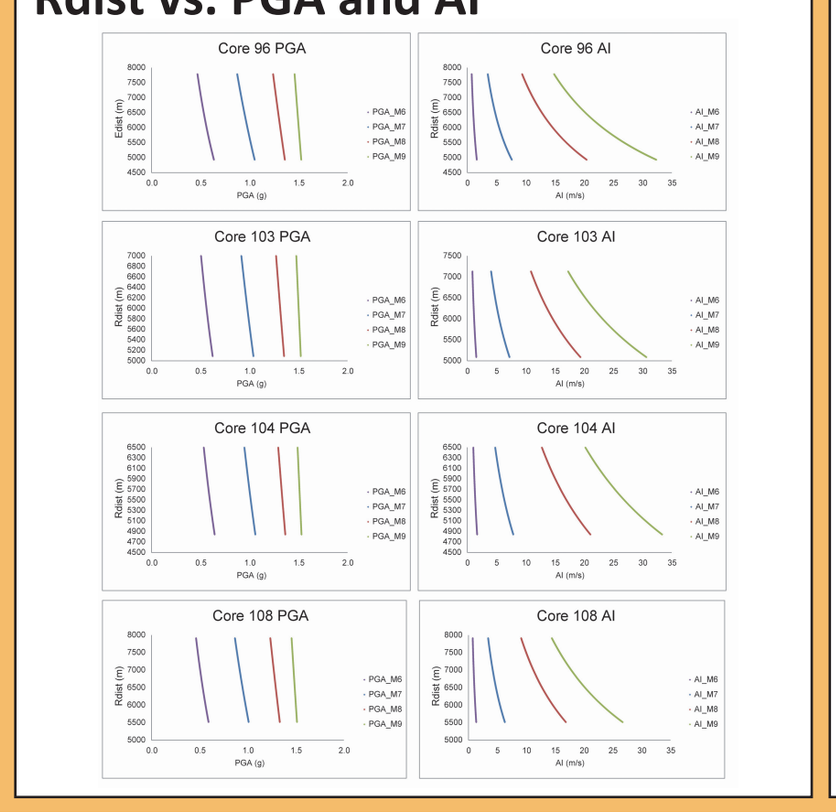

Ground motion contributions to core site source areas

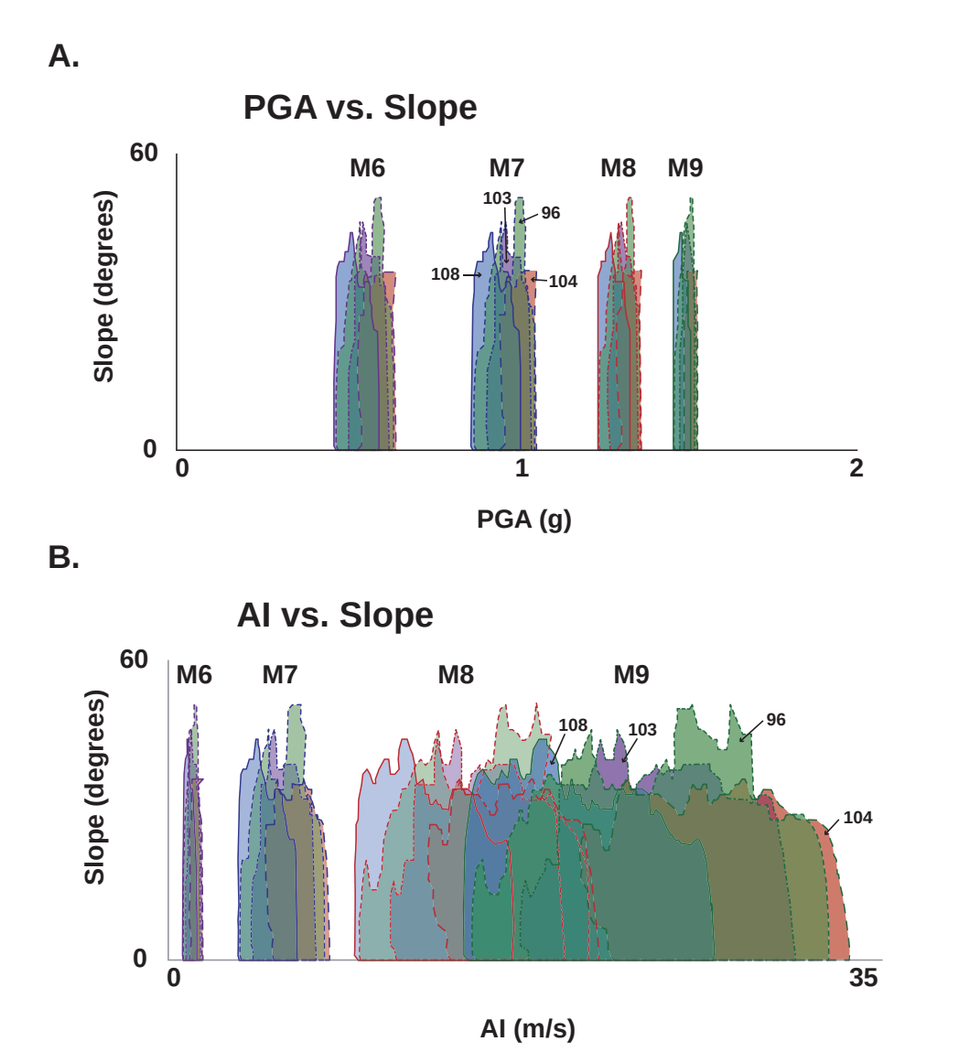

We plot envelopes of A. PGA (g) and B. AI (m/s) versus slope (degrees) for four earthquake magnitudes M = 6, 7, 8, and 9 with purple, blue, red, and green outlines respectively. We use different line symbols for four slope cores 96, 103, 104, and 108 with fill colors green, purple, red, and blue respectively.

Sorensen PGA (g) vs. slope and Rdist

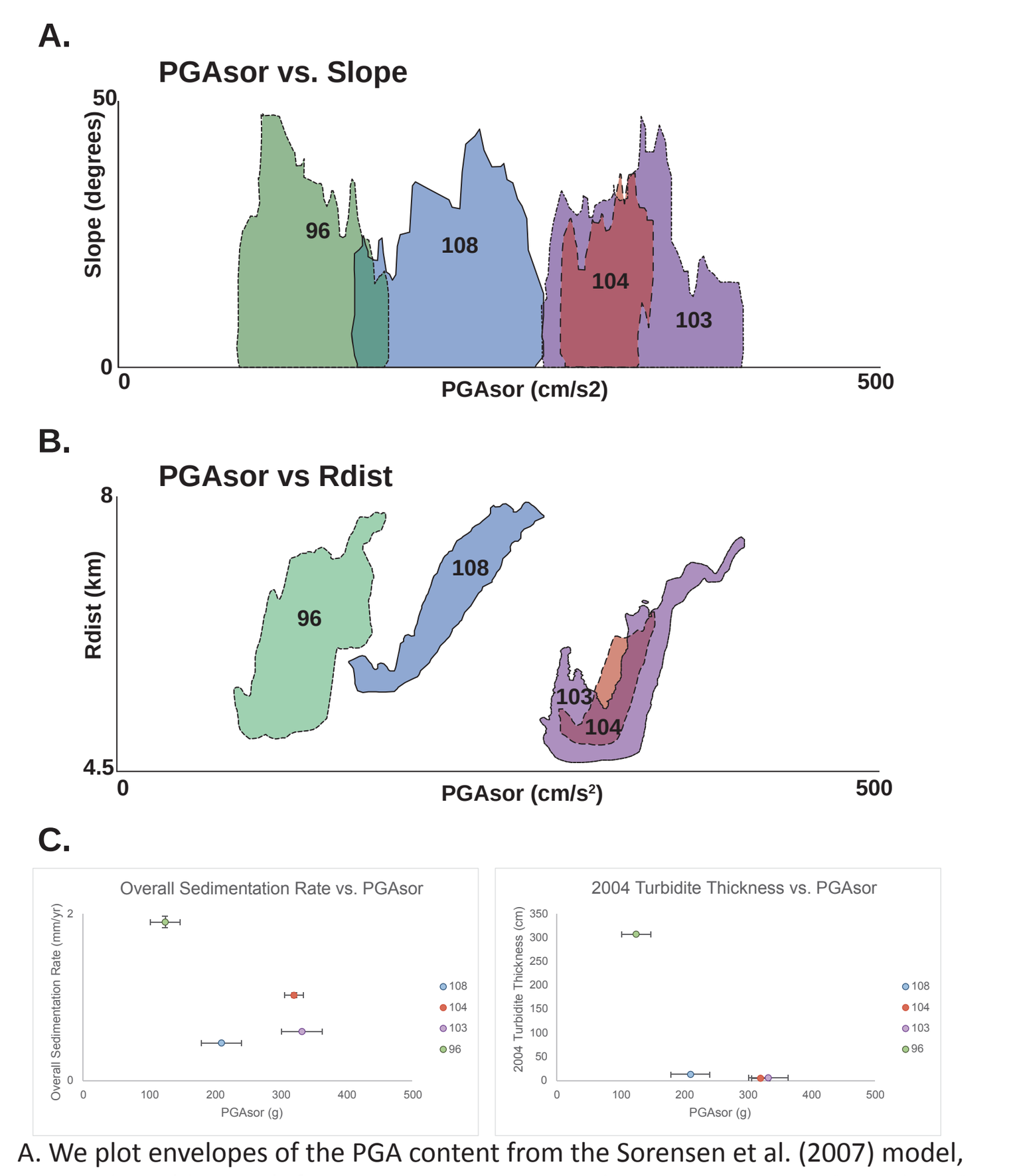

A. We plot envelopes of the PGA content from the Sorensen et al. (2007) model, versus slope (degrees), for cores 96, 103, 104, and 108 in green, purple, red, and blue respectively. B. We plot PGA content from Sorensen et al. (2007) versus Rdist (m). C. Overall sedimentation rate (mm per year) and 2004 turbidite thickness (cm) versus PGA modeled by Sorensen et al. (2007).

References:

Abrahamson, N. A., Gregor, N. J., and Addo, K., 2015, BC Hydro Ground Motion Prediction Equations For Subduction Earthquakes: Earthquake Spectra, p. in press.
Bronk Ramsey, C., 2009, Bayesian Analysis of Radiocarbon Dates: Radiocarbon, v. 51, no. 1, p. 337-360.
Chlieh, M., Avouac, J.-P., Hjorleifsdottir, V., Song, T.-R. A., Ji, C., Sieh, K., Sladen, A., Hebert, H., Prawirodirdjo, L., Bock, Y., and Galetzka, J., 2007, Coseismic Slip and Afterslip of the Great (Mw 9.15) Sumatra-Andaman Earthquake of 2004: Bulletin of the Seismological Society of America v. 97, no. 1A, p. S152-S173.
Fujino, S., Naruse, H., Matsumoto, D., Jarupongsakul, T., Sphawajruksakul, A., and Sakakura, N., 2009, Stratigraphic evidence for pre-2004 tsunamis in southwestern Thailand: Marine Geology, v. 262, p. 25-28.
Gorum, T., Fan, X., van Westen, C. J., Huang, R. Q., Xu, Q., Tang, C., and Wang, G., 2011, Distribution pattern of earthquake-induced landslides triggered by the 12 May 2008 Wenchuan earthquake: Geomorphology, v. 133, p. 152-167.
Grand Pre, C., Horton, B., Kelsey, H., Rubin, C., Hawkes, A., Natawidjaja, D. H., Daryono, M., and Yulianto, E., 2008, Application of Microfossils to Reconstruct a Paleoseismic Record of the Sunda Subduction Megathrust, Northern Sumatra: EOos Trans. AGU, v. 89, no. 53.
Ishii, M., Shearer, P. M., Houston, H., and Vidale, J. E., 2005, Extent, duration and speed of the 2004 Sumatra-Andaman earthquake imaged by the Hi-Net array: Nature, v. 435, no. 7044, p. 933.
Jankaew, K., Atwater, B. F., Sawai, Y., Charoentitirat, T., Martin, M. E., and Prendergast, A., 2008, Medieval forewarning of the 2004 Indian Ocean tsunami in Thailand: Nature, v. 455, p. 1228-1231.
Jibson, R. W., 2009, Using Landslides for Paleoseismic Analysis, in McCalpin, J. P., ed., Paleoseismology, Volume 1: USA, Academic Press, p. 565-601.
Kanno, T., Narita, A., Morikawa, N., Fujiwara, H., and Fukushima, Y., 2006, A New Attenuation Relation for Strong Ground Motion in Japan Based on Recorded Data: BSSA, v. 96, no. 3, p. 879-897.
Keefer, D. K., 1984, Landslides caused by earthquakes: GSA Bulletin, v. 95, p. 406-421.
Meltzner, A. J., Sieh, K., Chiang, H., Shen, C., Suwargadi, B. W., Natawidjaja, D. H., Philibosian, B., Briggs, R. W., and Galetzka, J., 2010, Coral evidence for earthquake recurrence and an A.D. 1390–1455 cluster at the south end of the 2004 Aceh–Andaman rupture: Journal of Geophysical Research, v. 115, no. B10402, p. 1-46.
Meltzner, A. J., Sieh, K., Chiang, H.-W., Shen, C.-C., Suwargadi, B. W., Natawidjaja, D. H., Philibosian, B., and Briggs, R. W., 2012, Persistent termini of 2004- and 2005-like ruptures of the Sunda megathrust: Journal of Geophysical Research, v. 117, no. B004405, p. 15.
Monecke, K., Finger, W., Klarer, D., Kongo, W., McAdoo, B., Moore, A., and Sudrajat, S., 2008, A 1,000-year sediment record of tsunami recurrence in northern Sumatra: Nature, v. 455, p. 1232-1234.
Rajendran, C. P., Rajendran, K., Anu, R., Earnest, A., Machado, T., Mohan, P. M., and Freymueller, J., 2007, Crustal Deformation and Seismic History Associated with the 2004 Indian Ocean Earthquake: A Perspective from the Andaman–Nicobar Islands: BSSA, v. 97, no. 1A, p. S174-S191.
Rajendran, K., Rajendran, C. P., Earnest, A., Ravi Prasad, G. V., Dutta, K., Ray, D. K., and Anu, R., 2008, Age estimates of coastal terraces in the Andaman and Nicobar Islands and their tectonic implications: Tectonophysics, v. 455, p. 52-60.
Reimer, P. J., Baillie, M. G. L., Bard, E., Bayliss, A., Beck, J. W., Bertrand, C. J. H., Blackwell, P. G., Ramsey, C. B., Buck, C. E., Burr, G. S., Edwards, R. L., Friedrich, M., Grootes, P. M., Guilderson, T. P., Hajas, I., Heaton, T. J., Hogg, A. G., Hughen, K. A., Kaiser, K. F., Kromer, B., McCormac, F. G., Manning, S. W., Reimer, R. W., Richards, D. A., Southon, J. R., Talamo, S., van der Plicht, J., and Weyhenmeyer, C. E., 2009, INTCAL09 and MARINE09 Radiocarbon Age Calibration Curves, 0–50,000 Years cal BP: Radiocarbon, v. 51, no. 4, p. 1111-1150.
Reimer, P. J., Bard, E., Bayliss, A., Beck, J. W., Blackwell, P. G., Ramsey, C. B., Grootes, P. M., Guilderson, T. P., Haflidason, H., Hajdas, I., Hatté, D., Heaton, T. J., Hoffman, D. L., Hogg, A. G., Hughen, K. A., Kaiser, K. F., Kromer, B., Manning, S. W., Niu, M., Reimer, R. W., Richards, D. A., Scott, E. M., Southon, J. R., Staff, R. A., Turney, C. S. M., and Van der Plicht, J., 2013, IntCal13 and Marine13 Radiocarbon Age Calibration Curves 0–50,000 Years cal BP: Radiocarbon, v. 55, no. 4, p. 1869-1887.
Rhodes, E. J., Bronk Ramsey, C., Outram, Z., Batt, C., Willis, L., Dockrill, S., and Bond, J., 2003, Bayesian methods applied to the interpretation of multiple OSL dates: high precision sediment ages from Old Scatness Broch excavations, Shetland Isles: Quaternary Science Reviews, v. 22, no. 10-13, p. 1231-1244.
Sorensen, M. B., Atakan, K., and Pulido, N., 2007, Simulated Strong Ground Motions for the Great M 9.3 Sumatra–Andaman Earthquake of 26 December 2004: BSSA, v. 97, no. 1A, p. S139-S151.
Stein, S., and Okal, E., 2007, Ultralong Period Seismic Study of the December 2004 Indian Ocean Earthquake and Implications for Regional Tectonics and the Subduction Process: BSSA, v. 97, no. 1A, p. S279-S295.
Stuiver, M., and Reimer, P. J., 1986, A computer program for radiocarbon age calibration: Radiocarbon, v. 28, p. p. 1022-1030.
Stuiver, M., Reimer, P. J., and Braziunas, T. F., 1998, High precision radiocarbon age calibration for terrestrial and marine samples: Radiocarbon, v. 40, no. 3, p. 1127-1151.
Sumner, E. J., Siti, M., McNeil, L. C., Talling, P. J., Henstock, T., Wynn, R., Djadjadihardja, Y., and Permana, H., 2013, Can turbidites be used to reconstruct a paleoearthquake record for the central Sumatran margin?: Geology, v. 41, p. 763-766.
Tolstoy, M., and Bohnenstiehl, D. R., 2006, Hydroacoustic contributions to understanding the December 26th 2004 great Sumatra–Andaman Earthquake: Survey of Geophysics, v. 27, p. 633-646.
Travasarou, T., Bray, J. D., and Abrahamson, N. A., 2003, Empirical attenuation relationship for Arias Intensity: Earthquake Engineering and Structural Dynamics, v. 32, p. 1133-1155.
Yagi, Y., 2004, Preliminary results of rupture process for 2004 off coast of Northern Sumatra giant earthquake, Volume 2013: International Institute of Seismology and Earthquake Engineering.
Zhao, J. X., and Xu, H., 2012, Magnitude-Scaling Rate in Ground-Motion Prediction Equations for Response Spectra from Large Subduction Interface Earthquakes in Japan: BSSA, v. 102, no. 1, p. 222-235.
Zhao, J. X., Zhang, J., Asano, A., Ohno, Y., Oouchi, T., Takahashi, T., Ogawa, H., Irikura, K., Thio, H. K., Somerville, P. G., Fukushima, Y., and Fukushima, Y., 2006, Attenuation Relations of Strong Ground Motion in Japan Using Site Classification Based on Predominant Period: BSSA, v. 96, no. 3, p. 898-913.